Earth and Planetary Science Letters 431 (2015) 119–126

Contents lists available at ScienceDirect

Earth and Planetary Science Letters

www.elsevier.com/locate/epsl

Distinctly different parental magmas for calc-alkaline plutons and tholeiitic lavas in the central and eastern Aleutian arc

Yue Cai [a,*], Matthew Rioux [b], Peter B. Kelemen [a,c], Steven L. Goldstein [a,c], Louise Bolge [a], Andrew R.C. Kylander-Clark [d]

[a] Lamont-Doherty Earth Observatory of Columbia University, 61 Rt. 9W, Palisades, NY, 10964, USA
[b] Earth Research Institute, University of California, Santa Barbara, CA, 93106, USA
[c] Department of Earth and Environmental Sciences, Columbia University, 61 Rt. 9W, Palisades, NY, 10964, USA
[d] Department of Earth Science, University of California, Santa Barbara, CA, 93106, USA

ARTICLE INFO

Article history:
Received 23 April 2015
Received in revised form 23 July 2015
Accepted 25 July 2015
Available online xxxx
Editor: A. Yin

Keywords:
continental crust formation
plutons
convergent margin
isotope tracers
subduction processes

ABSTRACT

Cenozoic calc-alkaline plutons that comprise the middle crust of the central and eastern Aleutians have distinct isotopic and elemental compositions compared to Holocene tholeiitic lavas in the same region, including those from the same islands. Therefore the Holocene lavas are not representative of the net magmatic transfer from the mantle into the arc crust. Compared to the lavas, the Eocene to Miocene (9–39 Ma) intermediate to felsic plutonic rocks show higher SiO_2 at a given Fe/Mg ratio, and have higher εNd–εHf values and lower Pb–Sr isotope ratios. However, the plutonic rocks strongly resemble calc-alkaline Holocene volcanics with more "depleted" isotope ratios in the western Aleutians, whose composition has been attributed to significant contributions from partial melting of subducted basaltic oceanic crust. These data could reflect a temporal variation of central and eastern Aleutian magma source compositions, from predominantly calc-alkaline compositions with more "depleted" isotope ratios in the Paleogene, to tholeiitic compositions with more "enriched" isotopes more recently. Alternatively, the differences between central Aleutian plutonic and volcanic rocks may reflect different transport and emplacement processes for the magmas that form plutons versus lavas. Calc-alkaline parental magmas, with higher SiO_2 and high viscosity, are likely to form plutons after extensive mid-crustal degassing of initially high water contents. This conclusion has overarching importance because the plutonic rocks are chemically similar to bulk continental crust. Formation of similar plutonic rocks worldwide may play a key role in the genesis and evolution of continental crust.

1. Introduction

Arc magmatism is the most important process that generates continental crust today and probably throughout Earth history. It is commonly inferred that compositions of primitive arc lavas are representative of the bulk composition of arc crust (e.g., Rudnick and Fountain, 1995; Tatsumi et al., 2008). However, the composition of average arc lavas is basaltic, while the bulk continental crust is andesitic with high molar Mg/(Mg + Fe) ratio or Mg# (e.g., Taylor and McLennan, 1995; Rudnick and Fountain, 1995; Rudnick and Gao, 2003; Kelemen et al., 2003b, 2014). Many hypotheses have been proposed to resolve this discrepancy, such as lower crustal foundering (Herzberg et al., 1983; Arndt and Goldstein, 1989; Kay and Kay, 1991); crustal formation from primary mantle-derived andesitic magmas (Kelemen, 1995); mixing of basaltic rock with silicic magma derived by partial melting of mafic, subducting crust (Martin, 1986); relamination of felsic, differentiated subducted crustal material (Hacker et al., 2011) and fractionation of water-rich magmas at moderate to high pressure conditions (Sisson and Grove, 1993; Grove et al., 2003; Jagoutz et al., 2011). A key aspect of several of these hypotheses is that the compositions of the largely unsampled plutonic arc middle crust may differ from the erupted arc lavas, and instead more closely resemble the continental crust (e.g., Perfit et al., 1980; Kay et al., 1990).

Low seismic wave-speeds suggest that plutonic arc middle crust may be more silicic than surficial volcanic rocks in some arcs (e.g. Suyehiro et al., 1996; Tatsumi et al., 2008). Similarly, combined geobarometry and geochemistry for the Mesozoic Talkeetna and Kohistan intra-oceanic arc sections show that felsic rocks are abundant in the middle crust, and that the crustal bulk composition may have been andesitic rather than basaltic (Behn and Kelemen, 2006; Hacker et al., 2008; Jagoutz and Schimdt, 2012;

* Corresponding author.
E-mail addresses: cai@ldeo.columbia.edu, merrycai@gmail.com (Y. Cai).

http://dx.doi.org/10.1016/j.epsl.2015.07.058
0012-821X/

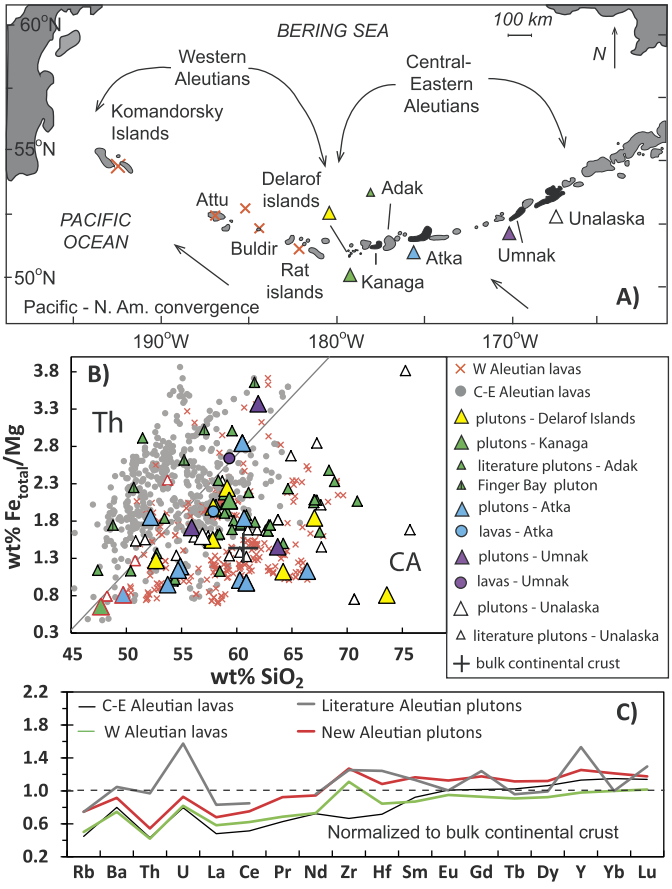

Fig. 1. A) Schematic map of the Aleutian island arc, sampled areas are highlighted in black. B) Wt% SiO_2 versus Fe/Mg ratio of studied Aleutian magmas and literature data downloaded from the GEOROC database (http://georoc.mpch-mainz.gwdg.de; Sarbas, 2008). By convention, the Fe/Mg ratio is calculated using wt% MgO and FeO, with all Fe as FeO. The bulk continental crust composition is from Rudnick and Gao (2003). A complete list of references for the literature data is provided in the Supplementary Materials. Samples with Eu/Eu* > 1 are outlined in red (the calculation is given in the Fig. 2). C) Average trace element compositions of Aleutian plutons and lavas are fractionation corrected to Mg# = 0.5 following Behn and Kelemen (2006) and normalized to the composition of bulk continental crust (Rudnick and Gao, 2003). Extended trace element patterns are shown in Fig. S2. (For interpretation of the references to color in this figure legend, the reader is referred to the web version of this article.)

Rioux et al., 2010). In the Aleutian arc, seismic data require a mafic bulk composition for the arc lower crust (Holbrook et al., 1999; Fliedner and Klemperer, 1999; Shillington et al., 2004); however, the upper and middle crust in the Aleutians contain abundant intermediate composition plutons (e.g., Kay et al., 1982, 1990; Kay and Kay, 1994; Perfit et al., 1980; Yogodzinski et al., 1993).

This paper reports new data on plutonic rocks (and two lavas) from the central and eastern Aleutian arc, and compares them with the large existing dataset on Holocene Aleutian volcanics. We define the central and eastern Aleutians as east of 180° W, which includes the oceanic arc extending from the western end of the Alaska Peninsula to the Delarof Islands; and the western Aleutians as west of 180° W, which includes the active arc extending from the Rat Islands west to the Komandorsky Islands and adjacent submarine volcanoes (Fig. 1A). In order to constrain the composition and timing of plutonism, we report results from whole rock major and trace elements; Sm–Nd, Rb–Sr and Lu–Hf isotopic analyses; and U–Pb zircon geochronology.

2. Methods

Zircon U–Pb geochronology was conducted by laser ablation on a Nu plasma multi-collector ICP-MS at the University of California at Santa Barbara (UCSB), following the procedures described in Kylander-Clark et al. (2013). Reported $^{206}Pb/^{238}U$ dates are Th- and common Pb-corrected, as described in the U–Pb zircon geochronology methods and data interpretations sections of the Supplementary Material (Table S2, Text S1).

All other geochemical analyses were carried out at Lamont-Doherty Earth Observatory (LDEO). Major element analyses were carried out using an Agilent ICP-OES on rock powders digested with $Li_2B_4O_7$ flux fusion. Trace element analyses were carried out on a VG PlasmaQuad ExCell quadrupole ICP-MS on rock powders digested using both hotplate HF-HNO_3 acid digestion (Ba, U, Th, Rb, Sr, Li, Ce, Pb, Nb, Ta) and Na_2O_2 sintering (La, Nd, Sm, Eu, Pr, Zr, Hf, Tb, Gd, Dy, Yb, Lu, Y) to ensure complete digestion of zircons and other accessory minerals following procedures outlined in Meisel et al. (2002). Pb–Sr–Nd isotope analyses were carried out on acid leached and hotplate digested samples. Hf isotope analyses were carried out on both hotplate digested samples and sintered samples. A comparison of the effects of hotplate digestions and sintering demonstrated its importance for elements such as Zr and Hf, and for Hf isotopes in older samples. Details, and the data, are in the Supplementary Materials (Tables S1–S5, Text S2).

Nd, Pb, Hf, and Sr isotopes were measured on a ThermoScientific Neptune Plus multi-collector MC-ICP-MS in static mode; some Sr isotope ratios were measured on a VG-Sector 54 TIMS in multi-dynamic mode (Table S1). The MC-ICP-MS instrumental drift is monitored by standard-sample bracketing using JNdi-1, a Johnson-Matthey lab Hf standard with Hf isotope ratios indistinguishable from JMC 475, NBS 987 Sr, and NBS 981 Pb. Typically 30–70 standards and 20–30 samples are analyzed during a 24-hr long run period, and reported 2SD external errors reflect the reproducibility of the standards. Reported values are corrected to those of the international standards. Quality control was further evaluated through measurements of the La Jolla Nd solution standard, and rock standards BCR-2 and BHVO-2. The analytical metadata (standards data, amounts per sample, signal intensities, values used for international standards, results, and reproducibility) are listed in Table S5. Hf isotope ratios are often listed as εHf, even on modern day and recent samples, therefore we do so here, where the deviation is in parts per 10,000 from a "Chondritic Uniform Reservoir" (CHUR) value ($^{176}Hf/^{177}Hf_{CHUR} = 0.282785$, Bouvier et al., 2008), and also for Nd isotope ratios (where $^{143}Nd/^{144}Nd_{CHUR} = 0.512638$, Jacobsen and Wasserburg, 1980).

3. Results

Weighted mean laser ablation-ICP-MS Th-corrected $^{206}Pb/^{238}U$ ages of the plutonic samples range from 9.20 ± 0.04 to 39.1 ± 0.2 Ma (Eocene to Miocene), which means they are older than lavas from the same region that have been the focus of most previous studies. The plutonic rocks are predominantly calc-alkaline. They show higher average SiO_2 and higher trace element concentrations than lavas from the same region at a given Fe/Mg ratio (calculated using wt% MgO and FeO, with all Fe as FeO) (Fig. 1A–C). The major and trace element compositions of the studied plutonic rocks resemble lavas from the western Aleutians, as well as estimates for the bulk continental crust (Fig. 1B–C). Except for two samples, the plutonics show negligible Eu anomalies. They have similar or higher Na + K (mol%), and similar or lower CaO and Al_2O_3 (wt%) at a given Mg# compared to the lavas (Fig. 2). These data suggest that the plutonic rocks represent fully crystallized magmas, rather than crystal cumulates resulting from partial crystallization followed by removal of evolved melt. The two samples

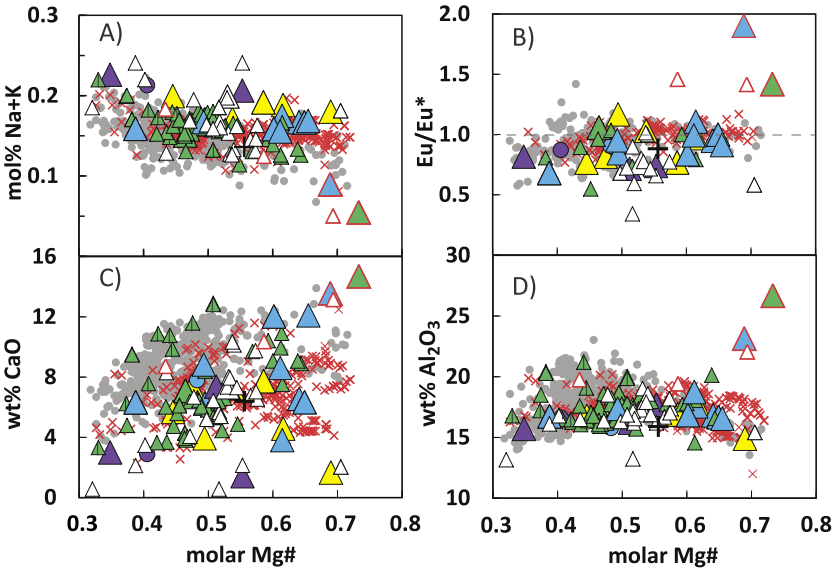

Fig. 2. Selected major and trace element compositions versus molar Mg# of Aleutian plutons and lavas, showing that the Eocene–Miocene plutonic rocks resemble western Aleutian lavas and match better with the continental crust than Holocene central and eastern Aleutian lavas. Molar Mg# = molar MgO/(molar MgO + molar FeO), with all Fe as FeO. Of the plutonics, only two of our studied samples and a few of the literature samples (outlined in red) show chemical signatures that indicate incorporation of cumulate plagioclase, such as elevated Al_2O_3 contents and "positive" Eu anomalies (Eu/Eu* > 1, where $Eu^* = Eu(N)/[\sqrt{Sm(N)*Gd(N)}]$ and elemental concentrations are normalized to chondrite compositions from McDonough and Sun, 1995). Overall, at a given Mg# the plutonic rocks show similar to higher mol% Na + K, and similar to lower wt% CaO than central and eastern Aleutian volcanics. (For interpretation of the references to color in this figure legend, the reader is referred to the web version of this article.)

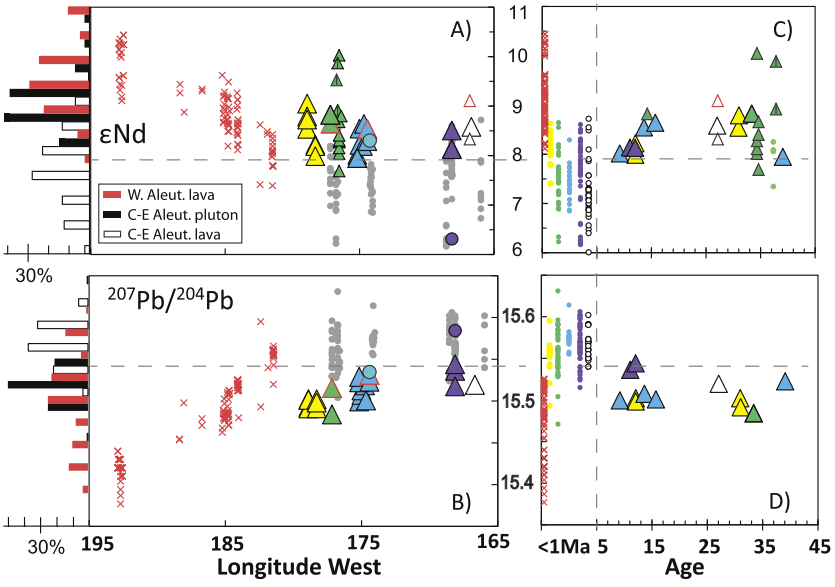

Fig. 3. Present-day Nd and Pb isotope ratios of Aleutian magmas vs. longitude (A and B) and vs. ages (C and D). Circles are central and eastern Aleutian volcanics (the two larger circles are from this study): Yellow = Rat and Delarof Islands, Green = Adak and Kanaga, Blue = Atka, Purple = Umnak, White = Unalaska. Error bars are smaller than the symbols. The other symbols are the same as in Fig. 1. In C) and D), the Holocene volcanics are separated by location only without age differences. (For interpretation of the references to color in this figure legend, the reader is referred to the web version of this article.)

with positive Eu anomalies (marked with red rims in the figures) show clear signatures of plagioclase accumulation (e.g., high Al). However, we include these samples in the following discussion because they have similar isotope compositions as other plutonic samples, and because plagioclase accumulation would not change the isotopic composition of the magma.

The Eocene–Miocene central and eastern Aleutian plutons show higher present-day εNd and εHf, and lower Pb isotope ratios than the Holocene volcanic rocks from the same area (Figs. 3 and 4). Age-corrected Sr isotope ratios in the plutonic samples are also generally lower than in Holocene lavas from the same islands (Fig. S4), though we place less weight on the Sr data due to the possible effects of alteration. The isotopic compositions of the plutonic rocks fall between the fields defined by central–eastern and western Aleutian lavas (Fig. 4). There is no clear temporal trend in Nd–Hf–Pb isotope compositions of Aleutian plutonic samples (Fig. 3). Without sintering, Hf isotope ratios and concentrations reflected incomplete digestion of zircons (shown in Supplementary Materials). After sintering, Nd–Hf isotope ratios lie close to the mantle crust array (Vervoort et al., 2011) and show negative

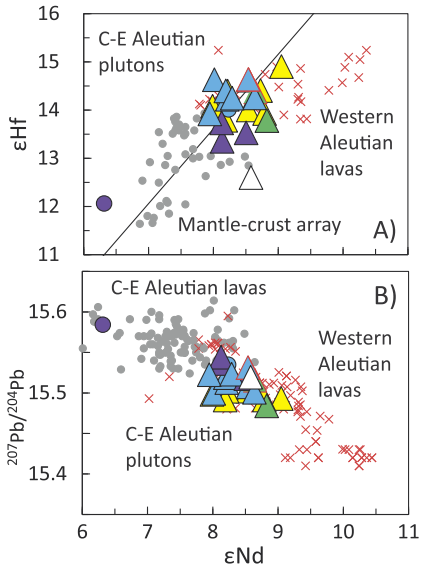

Fig. 4. A) and B) show present-day Nd, Pb, Hf isotopic compositions of Aleutian magmas. Central and eastern (C–E) Aleutian plutons fall between the fields defined by C–E Aleutian lavas and western Aleutian lavas. The εNd–εHf mantle–crust array is from Vervoort et al. (2011). The error bars are smaller than the symbols. The symbols are listed in Fig. 1.

correlations with Pb isotope ratios (Fig. 4). Age corrections do not change these relationships (Figs. S4–S5 and Table S4).

4. Discussion

4.1. Central–eastern Aleutian plutons and lavas are derived from distinct sources

This study is the first that demonstrates statistically significant and internally consistent differences in isotope and elemental compositions between lavas and the plutons in any arc. It has been shown previously that in the central and eastern Aleutians the erupted lavas are predominantly tholeiitic while the plutons are predominantly calc-alkaline (e.g., Kay, 1978; Kay et al., 1982; Kay and Kay, 1994; Fig. 4B in Kelemen et al., 2003a; Figs. 4 and 5 in Kelemen et al., 2003b, 2014), with the exception of the tholeiitic Finger Bay pluton on Adak Island. Isotopic differences between plutons and lavas have been inferred previously based on a small number of samples (Kay et al., 1986).

The differences in isotope signatures between the plutonic rocks studied here, and lavas from the same islands in the central and eastern Aleutians, demonstrate that the intrusive and extrusive suites in this area are derived from different sources. These isotopic differences cannot be explained by chemical differentiation or crustal assimilation, although these processes may affect some other compositional characteristics of Aleutian magmas.

Elevated parental magma water contents and oxygen fugacity can drive the differentiating magma towards the calc-alkaline trend by suppressing plagioclase fractionation and bringing oxide and amphibole fractionation closer to the liquidus (e.g., Sisson and Grove, 1993). This process is often called upon to explain coexisting calc-alkaline and tholeiitic arc magmas (e.g., Osborn, 1959; Gill, 1981, Sections 11.3 and 12.1; Grove et al., 2003, 2005; Zimmer et al., 2010; Jagoutz et al., 2011). However, it cannot explain the isotopic differences between the plutons and the lavas.

High εNd and εHf, and lower Pb isotope ratios might be generated via assimilation of arc crust or pre-existing oceanic crust (e.g. Kay and Kay, 1994). However, AFC (assimilation and fractional crystallization) modeling shows that to generate the isotopic compositions of the plutons via crustal assimilation requires large extents of fractionation (up to 90%, Fig. 5) and the resulting magma would have high Nd and Hf contents and strong negative Eu anomalies. These signatures are not observed in the plutonic rocks, which plot far above the AFC trend. Thus, the isotopic differences between the plutons and the lavas in the Aleutians were not generated through crustal assimilation.

One may also argue that the plutons could represent deeper crustal magma chambers that have experienced more mafic magmatic recharge (e.g. Lee et al., 2014), a process that could buffer the isotopic compositions of the magma towards "isotopically depleted" compositions (referring to Nd–Hf–Pb–Sr isotopic values that reflect long term depletions in incompatible elements, thus low Nd/Sm, Hf/Lu, U/Pb, Th/Pb and Rb/Sr). However, mafic magma recharge cannot explain the major element characteristics of the plutons. For example, compared to the volcanics, the plutons show elevated SiO_2 contents for a given Fe/Mg ratio (Fig. 1B) and lower MgO contents for a given Mg# (Fig. S6A). Additionally, mixing between more primitive, "isotopically depleted" magmas and more evolved, "isotopically enriched" magmas should generate negative correlations between Nd isotope ratios and SiO_2 and positive correlations between Nd isotopes and MgO, which is not the case for the plutons (Fig. S6 B–C). Instead, the isotopic differences between central–eastern Aleutian plutons and lavas persist across a large range of major element compositions.

4.2. Coeval formation of calc-alkaline and tholeiitic parental magmas?

Instead, we propose two alternative hypotheses based on the data presented. (1) The sources of central and eastern Aleutian magmas changed over time, with the early source characterized by "depleted" Nd, Hf and Pb isotope ratios, represented by the plutons, which are Miocene and older; changing to a present day source characterized by relatively more "enriched" Nd, Hf and Pb isotope ratios, represented by Holocene central and eastern Aleutian lavas. In this view, the isotopic shift was accompanied by a change in major element magma composition, from more calc-alkaline to more tholeiitic, perhaps due to decreasing SiO_2, fO_2, and/or H_2O contents in central–eastern Aleutian parental magmas over time. (2) The differences between plutonic and volcanic compositions reflect coeval input of distinct parental magma types from the mantle into the Aleutian crust. In this case, the dominance of calc-alkaline compositions among the plutons could reflect higher SiO_2, fO_2, and/or H_2O contents in their parental magmas, compared to the basaltic, more reduced magmas with lower H_2O contents that are parental to Aleutian tholeiitic lavas (Kay et al., 1990; Kelemen, 2003a, 2003b, 2014).

The scarcity of isotope data on pre-Holocene volcanics in the central and eastern Aleutian islands that host our plutonic samples means that we cannot definitively distinguish between these two hypotheses. However, the isotopic and geochronological data from the plutons do not show systematic temporal variations from 39 Ma to 9 Ma (Fig. 3C–D). If central and eastern Aleutian lavas and plutons have shared a common source composition through time, then the data require an abrupt change in the magma source between ~9 Ma and the Holocene, from predominantly calc-alkaline to predominantly tholeiitic. We are not aware of any large changes in the regional tectonics that would cause such a shift. Moreover, coeval calc-alkaline plutons and tholeiitic lavas are observed at Adak, where calc-alkaline plutons intrude ca. 38 Ma tholeiitic lavas, suggesting that the observed compositional differences between the plutons and the lavas have persisted through time (Jicha et al., 2006; Kay et al., 1983).

Therefore, we prefer the hypothesis that the distinct isotopic and geochemical signatures of the central and eastern Aleutian plutons and lavas reflect distinct, coeval magma sources. The observed differences may be generated by the addition of differ-

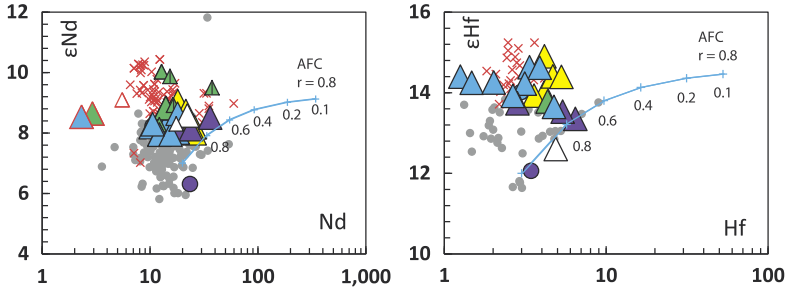

Fig. 5. AFC model showing the effect of assimilating arc crust or pre-existing oceanic crust, following DePaolo (1981), assuming $D_{Nd} = 0.06$, $D_{Hf} = 0.1$ (calculated assuming 50% plag, 25% cpx, 10% olivine and 10% opx, using Kd's from Salters and Stracke, 2004). Assimilated crust compositions are modeled as [Hf] = 2.5, εHf = 15; [Nd] = 10.6, εNd = 10. The blue lines show the evolution trend of the magma as the fraction (F) of the remaining melt decreases (F values are shown next to the tick marks along the AFC trend). Only $r = Ma/Mc = 0.8$ is shown, where Ma = mass assimilation rate and Mc = fractionation rate, following DePaolo (1981). Smaller r values would generate lower εNd and εHf values at a given F value. (For interpretation of the references to color in this figure legend, the reader is referred to the web version of this article.)

ent types and amounts of subducted material to calc-alkaline and tholeiitic magmas, mirroring the differences between western vs. central and eastern Aleutian lavas.

4.3. Central–eastern Aleutian plutons resemble western Aleutian calc-alkaline lavas

The oceanic part of the Aleutian arc has a well-defined, along-strike variation in Holocene lava compositions, ranging from dominantly calc-alkaline compositions with "depleted" Sr–Nd–Pb–Hf isotopic compositions in the western Aleutians, to tholeiitic compositions with more "enriched" isotopic compositions in the east (e.g., Kay and Kay, 1994; Kelemen et al., 2003a, 2003b; Singer et al., 2007). End-member western Aleutian lava compositions are primitive andesites and dacites showing light rare earth element (LREE) enrichment, heavy REE (HREE) depletion, and high Mg# (>0.6), Ni (>150 ppm) and Sr/Nd (>100). These can be understood as the result of reaction of mantle peridotite and hydrous, low degree partial melts of subducted material that formed in eclogite facies (e.g., Kay, 1978; Yogodzinski et al., 1995, 2001, 2015; Yogodzinski and Kelemen, 1998, 2007; Kelemen and Yogodzinski, 2007). A quantitative model of the reaction process is given in Kelemen et al. (2003a). Primitive calc-alkaline high Mg# andesites and dacites with strong adakitic signatures are found erupted through thin oceanic lithosphere in the western Aleutians, rendering it unlikely that deep crustal assimilation is responsible for their characteristic compositional signatures (Yogodzinski et al., 2015).

Western Aleutian lavas have the highest Nd and lowest Pb isotope ratios of any arc magmas worldwide (Kelemen et al., 2003a, 2003b, 2014; Singer et al., 2007; Yogodzinski et al., 2010, 2015). Both western Aleutian lavas and the plutonic rocks from the central and eastern Aleutians show high εNd and εHf values (Fig. 6) coupled with higher Th/Nd and Hf/Lu ratios than the "depleted MORB mantle" (DMM) source for mid-ocean ridge basalts (e.g., Salters and Stracke, 2004). These compositional characteristics, that is high Nd–Hf isotope ratios and incompatible element enrichment, are consistent with addition of low degree partial melts of subducted material in eclogite facies, where garnet and omphacite preferentially retain Lu and Nd in the solid residue compared to Hf and Th, respectively (e.g., Cai et al., 2014; Kay, 1978; Klemme et al., 2002; Yogodzinski et al., 2015).

The eclogite melt component derived from the subducted material could comprise ~20% of the parental magma for western Aleutian primitive andesites and dacites (Fig. 6, and Kelemen et al., 2003a; Yogodzinski et al., 2015). The SiO_2-rich nature of this component poses a bit of a conundrum. The high Mg# and Ni contents of the primitive andesites and dacites suggest extensive interaction with mantle olivine, which should limit SiO_2 contents of the resulting magmas to <60 wt% depending on pressure, alkali content, and H_2O content (Carroll and Wyllie, 1989; Draper and Green, 1999). Furthermore, reaction with the hot mantle wedge might be expected to raise MgO contents, whereas primitive Aleutian dacites have <5 wt% MgO despite their high Mg#'s. One possible explanation is that reacting eclogitic melts rise in cold diapirs that pond just beneath the crust and evolve by combined reaction and crystal fractionation in the shallow mantle (e.g., Gerya and Yuen, 2003; Kelemen et al., 2003b; Ringwood and Green, 1966). Instead or in addition, hydrous, high SiO_2 eclogite melts may be sufficiently abundant to convert some regions of the sub-arc mantle from peridotite to olivine-free pyroxenite by overwhelming the olivine–pyroxene SiO_2 buffer (Macpherson et al., 2006; Yogodzinski et al., 1994). Independent of the cause, the link between a substantial eclogite melt component and primitive andesites and dacites seems clear, not only in the western Aleutians but worldwide (e.g. Cai et al., 2014; Defant and Drummond, 1990; Kay, 1978; Shimoda et al., 1998; Stern and Kilian, 1996; Straub et al., 2011).

The calc-alkaline nature of western Aleutian lavas suggests high magmatic water contents. Zimmer et al. (2010) and Ruscitto et al. (2010) demonstrated a correlation between high H_2O content and strongly calc-alkaline magma series in the Aleutians and the Cascades. It is possible that calc-alkaline magma series also have higher fO_2 in their parental liquids, compared to tholeiitic magma series. Thus, we infer that parental magmas for typical western Aleutian primitive andesites and dacites likely have higher SiO_2, H_2O and fO_2 compared to parental magmas for typical central and eastern Aleutian tholeiitic basalts.

In comparison, central and eastern Aleutian volcanics have lower εNd and εHf values, and higher Sr and Pb isotope ratios, all of which are consistent with incorporation of a subducted sediment component similar to near-trench sediments sampled at DSDP Site 183 (Fig. 6 and Peucker-Ehrenbrink et al., 1994). The sediment component in the central and eastern Aleutian lavas is thought to contribute just a few percent of the mass of the parental magmas, with the balance coming from fluxed melting of the mantle wedge (Class et al., 2000; Kay et al., 1978; Miller et al., 1994; Singer et al., 2007). The isotopic signals associated with this sediment component are much weaker in western Aleutian lavas and systematically decrease with distance west of Adak (Kelemen et al., 2003a; Yogodzinski et al., 2015).

4.4. Calc-alkaline magmas may preferentially form plutons

If the distinct chemical and isotopic compositions of the plutonic and volcanic rocks in the central and eastern Aleutians are related to the addition of different types and amounts of subducted material, the intrusive versus extrusive nature of the lavas are likely also related to different transport mechanisms. Based on the major element and isotopic characteristics, the parental magmas are similar in the central and eastern Aleutian plutonic

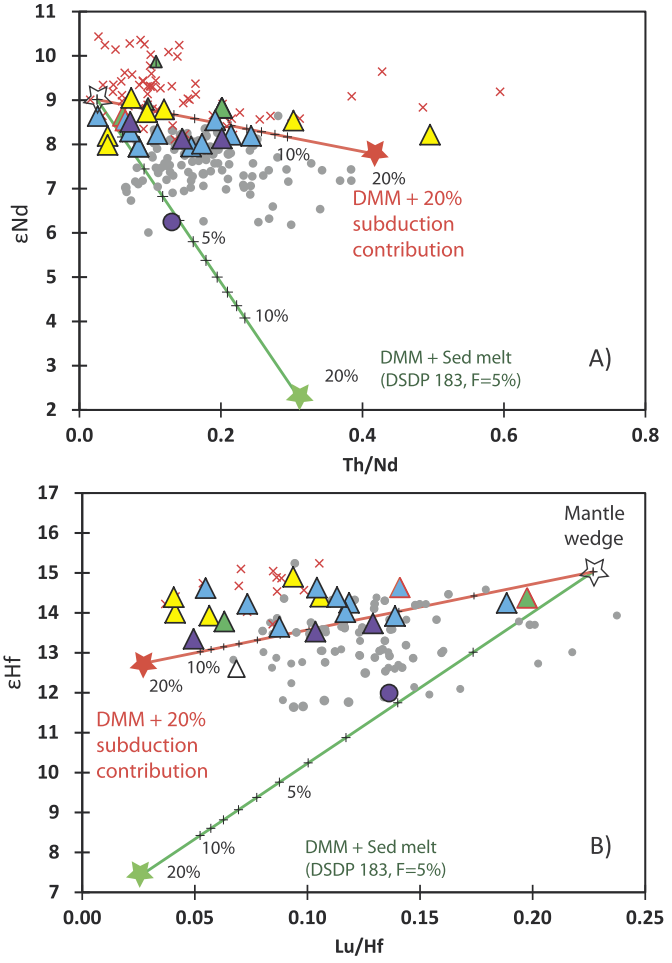

Fig. 6. Model results of different slab contributions for: (A) εNd vs. Th/Nd and (B) εHf vs. Lu/Hf. Green lines show the effect of adding sediment melt to the subarc mantle wedge; red lines show addition of partial melt of the subducted oceanic crust (F = 0.5%) and subducted sediments (F = 5%) in a 4:1 ratio. Partial melt of subducted oceanic crust is modeled as a 0.5% equilibrium melt of the average MORB (EPR north of the equator segment average, Gale et al., 2013). Sediment melt is modeled as a 5% equilibrium partial melt of DSDP 183 sediments (Plank, 2014). For slab melts, we assumed $D_{Th} = 0.2$, $D_{Nd} = 1.4$, $D_{Hf} = 0.5$, $D_{Lu} = 50$ (Skora and Blundy, 2010). The mantle wedge is modeled as a spinel lherzolite that would generate typical EPR MORB via 10% equilibrium melting using D-values from Salters and Stracke (2004). After mixing the slab melt with the mantle wedge, the metasomatized mantle undergoes 15% equilibrium partial melting with spinel lherzolite D-values to generate the mixing lines shown in the figure (Salters and Stracke, 2004). (For interpretation of the references to color in this figure legend, the reader is referred to the web version of this article.)

rocks and western Aleutian lavas. However, plutonics and lavas in central and eastern Aleutians have distinctly different parental magmas. Primitive (Mg# >0.6) andesites and dacites in the western Aleutians have low MgO, indicative of low melt-mantle equilibration temperatures, whereas primitive basalts in the central and eastern Aleutians have higher MgO, indicative of high melt-mantle equilibration temperatures. Magmas with high SiO_2 and H_2O become viscous, and preferentially stall during mid-crustal degassing (e.g., Cann, 1970). It is reasonable to infer that in the central and eastern Aleutians, such magmas predominantly stall to form the calc-alkaline plutons, rather than erupting as previously proposed (e.g., Kay et al., 1990; Kay and Kay, 1994; Kelemen et al., 2003a). In the thinner, faulted crust of the western Aleutians, such magmas erupt to form many small cones on the seafloor. In contrast, the parental magmas to central and eastern Aleutian tholeiitic lavas likely have higher temperatures and lower SiO_2 and H_2O contents. Such lower viscosity magmas may readily erupt.

If it turns out that parental magmas for both calc-alkaline and tholeiitic magma series are simultaneously present in the Holocene central and eastern Aleutian arc, then hot, parental tholeiites from the core of the mantle wedge may form conduits that "pierce through" shallow mantle pyroxenites and ponded parental calc-alkaline magmas during relatively rapid ascent to the surface. Such a process in arcs worldwide would result in the bulk arc crust having higher SiO_2 than erupted arc volcanics. This has important implications for our understanding of continent formation, since arc lavas are routinely used to estimate the average composition of magmas passing from the mantle into arc crust (e.g., Plank and Langmuir, 1993; Plank et al., 2002), and the bulk composition of arc crust (e.g., Tatsumi, 2000; Tatsumi et al., 2008).

5. Conclusions

In summary, Eocene to Miocene plutonic rocks in the central and eastern Aleutians show stronger calc-alkaline signatures than Holocene volcanics from the same region, and are similar to Holocene volcanics from the western Aleutians. The central and eastern Aleutian plutonics have higher εNd and εHf, and lower Pb and Sr isotope ratios than Holocene central and eastern Aleutian lavas. The isotopic signatures of the plutonic samples cannot be generated by crustal assimilation or magma fractionation in the Aleutians. Instead, they demonstrate distinct sources for the Holocene lavas and Cenozoic plutons in the central and eastern Aleutians. The parental magmas for the calc-alkaline plutons and lavas likely have higher SiO_2, H_2O and fO_2 than the parental magmas for tholeiitic lavas. This indicates that the major element differences between calc-alkaline and tholeiitic magma series in the central and eastern Aleutians arise, in part, from parental magmas with distinct initial compositions. The difference between central and eastern Aleutian lavas and plutonic rocks may reflect a temporal variation in the nature of parental magmas, or the effect of magma transport processes alone. More detailed studies of Aleutian plutons and pre-Holocene central and eastern Aleutian lavas are needed to resolve this uncertainty. However, the available evidence favors the hypothesis that the calc-alkaline magmas preferentially form plutons as they undergo a rapid viscosity increase during mid-crustal degassing. In contrast, dryer and hotter tholeiitic parental magmas with lower initial SiO_2 and H_2O contents preferentially erupt. Regardless of the cause, a first-order implication is that erupted magmas alone are not an accurate guide to the composition of the bulk arc crust. Furthermore, Aleutian plutonic rocks – and similar plutonic rocks worldwide – are compositionally similar to continental crust. Such plutons may be important building blocks for the continental crust. Understanding the processes of their formation is a key to understanding the genesis and evolution of the continents.

Acknowledgements

We thank Jean Hanley for careful preparation of the samples, Gwendolyn Hicks for enthusiastic assistance during her Federal work-study internship at Lamont, Jill Schneider for help with locating USGS field notes and other sample information, and Karen Benedetto for sorting out all the logistics. We are grateful to all the reviewers for their detailed and constructive comments which greatly helped us improve the manuscript. This study was funded by NSF OCE-1144759, NSF OCE-1144648 and EAR-1457293. This is LDEO contribution number 7922.

Appendix A. Supplementary material

Supplementary material related to this article can be found online at http://dx.doi.org/10.1016/j.epsl.2015.07.058.

References

Arndt, N.T., Goldstein, S.L., 1989. An open boundary between lower continental-crust and mantle – its role in crust formation and crustal recycling. Tectonophysics 161, 201–212.

Behn, M.D., Kelemen, P.B., 2006. Stability of arc lower crust: insights from the Talkeetna arc section, south central Alaska, and the seismic structure of modern arcs. J. Geophys. Res., Solid Earth 111, B11.

Bouvier, A., Vervoort, J.D., Patchett, P.J., 2008. The Lu–Hf and Sm–Nd isotopic composition of CHUR: constraints from unequilibrated chondrites and implications for the bulk composition of terrestrial planets. Earth Planet. Sci. Lett. 273, 48–57.

Cai, Y., LaGatta, A., Goldstein, S.L., Langmuir, C.H., Gómez-Tuena, A., Martín-del Pozzo, A.L., Carrasco-Núñez, G., 2014. Hafnium isotope evidence for slab melt contributions in the Central Mexican Volcanic Belt and implications for slab melting in hot and cold slab arcs. Chem. Geol. 377, 45–55.

Cann, J.R., 1970. Upward movement of granitic magma. Geol. Mag., 335–340.

Carroll, M.R., Wyllie, P.J., 1989. Experimental phase relations in the system tonalite–peridotite–H_2O at 15 kb: implications for assimilation and differentiation processes near the crust–mantle boundary. J. Petrol. 30, 1351–1382.

Class, C., Miller, D.M., Goldstein, S.L., Langmuir, C.H., 2000. Distinguishing melt and fluid subduction components in Umnak Volcanics, Aleutian Arc. Geochem. Geophys. Geosyst. 1.

Defant, M.J., Drummond, M.S., 1990. Derivation of some modern arc magmas by melting of young subducted lithosphere. Nature 347 (6294), 662–665.

DePaolo, D.J., 1981. Trace element and isotopic effects of combined wallrock assimilation and fractional crystallization. Earth Planet. Sci. Lett. 53, 189–202.

Draper, D.S., Green, T.H., 1999. P–T phase relations of silicic, alkaline, aluminous liquids: new results and applications to mantle melting and metasomatism. Earth Planet. Sci. Lett. 170 (3), 255–268.

Fliedner, M.M., Klemperer, S.L., 1999. Structure of an island-arc: wide-angle seismic studies in the eastern Aleutian Islands, Alaska. J. Geophys. Res., Solid Earth 104, 10667–10694.

Gale, A., Dalton, C.A., Langmuir, C.H., Su, Y., Schilling, J.-G., 2013. The mean composition of ocean ridge basalts. Geochem. Geophys. Geosyst. 14, 489–518.

Gerya, T.V., Yuen, D.A., 2003. Rayleigh–Taylor instabilities from hydration and melting propel 'cold plumes' at subduction zones. Earth Planet. Sci. Lett. 212 (1–2), 47–62.

Gill, J.B., 1981. Orogenic Andesites and Plate Tectonics. Springer-Verlag, Berlin, Heidelberg. 392 pp.

Grove, T.L., Elkins-Tanton, L.T., Parman, S.W., Chatterjee, N., Muntener, O., Gaetani, G.A., 2003. Fractional crystallization and mantle-melting controls on calc-alkaline differentiation trends. Contrib. Mineral. Petrol. 145, 515–533.

Grove, T.L., Baker, M.B., Price, R.C., Parman, S.W., Elkins-Tanton, L.T., Chatterjee, N., Muntener, O., 2005. Magnesian andesite and dacite lavas from Mt. Shasta, northern California: products of fractional crystallization of H_2O-rich mantle melts. Contrib. Mineral. Petrol. 148, 542–565.

Hacker, B.R., Mehl, L., Kelemen, P.B., Rioux, M., Behn, M.D., Luffi, P., 2008. Reconstruction of the Talkeetna intraoceanic arc of Alaska through thermobarometry. J. Geophys. Res. 113, B3.

Hacker, B.R., Kelemen, P.B., Behn, M.D., 2011. Differentiation of the continental crust by relamination. Earth Planet. Sci. Lett. 307, 501–516.

Herzberg, C.T., Fyfe, W.S., Carr, M.J., 1983. Density constraints on the formation of the continental Moho and crust. Contrib. Mineral. Petrol. 84, 1–5.

Holbrook, W.S., Lizarralde, D., McGeary, S., Bangs, N., Diebold, J., 1999. Structure and composition of the Aleutian island arc and implications for continental crustal growth. Geology 27, 31–34.

Jagoutz, O., Muntener, O., Schmidt, M.W., Burg, J.P., 2011. The roles of flux- and decompression melting and their respective fractionation lines for continental crust formation: evidence from the Kohistan arc. Earth Planet. Sci. Lett. 303, 25–36.

Jagoutz, O., Schmidt, M.W., 2012. The formation and bulk composition of modern juvenile continental crust: the Kohistan arc. Chem. Geol. 298, 79–96.

Jicha, B.R., Scholl, D.W., Singer, B.S., Yogodzinski, G.M., Kay, S.M., 2006. Revised age of Aleutian Island Arc formation implies high rate of magma production. Geology 34 (8), 661–664.

Kay, R.W., 1978. Aleutian magnesian andesites: melts from subducted Pacific ocean crust. J. Volcanol. Geotherm. Res. 4, 117–132.

Kay, R.W., Sun, S.-S., Lee-Hu, C.N., 1978. Pb and Sr isotopes in volcanic rocks from the Aleutian Islands and Pribilof Islands, Alaska. Geochim. Cosmochim. Acta 42, 263–272.

Kay, R.W., Rubenstone, J.L., Kay, S.M., 1986. Aleutian terranes from Nd isotopes. Nature 322 (6080), 605–609.

Kay, R.W., Kay, S.M., 1991. Creation and destruction of the lower continental-crust. Geol. Rundsch. 80, 259–278.

Kay, S.M., Kay, R.W., Citron, G.P., 1982. Tectonic controls on tholeiitic and calc-alkaline magmatism in the Aleutian Arc. J. Geophys. Res. 87 (B5), 4051–4071.

Kay, S.M., Kay, R.W., Brueckner, H.K., Rubenstone, J.L., 1983. Tholeiitic Aleutian arc plutonism – the Finger Bay pluton, Adak, Alaska. Contrib. Mineral. Petrol. 82 (1), 99–116.

Kay, S.M., Kay, R.W., Citron, G.P., Perfit, M.R., 1990. Calc-alkaline plutonism in the intra-oceanic Aleutian arc, Alaska. In: Kay, S.M., Rapela, C.W. (Eds.), Geological Society of America Special Papers, vol. 241, pp. 233–256.

Kay, S.M., Kay, R.W., 1994. Aleutian magmas in space and time. In: Plafker, G., Berg, H.C. (Eds.), The Geology of Alaska, vol. G-1. Geological Society of America, pp. 687–722.

Kelemen, P.B., 1995. Genesis of high Mg# andesites and the continental crust. Contrib. Mineral. Petrol. 120, 1–19.

Kelemen, P.B., Yogodzinski, G.M., Scholl, D.W., 2003a. Along-strike variation in lavas of the Aleutian island arc: implications for the genesis of high Mg# andesite and the continental crust. In: Eiler, J.M. (Ed.), Inside the Subduction Factory. In: AGU Monograph, vol. 138, pp. 224–276.

Kelemen, P.B., Hanghøj, K., Greene, A.R., 2003b. One view of the geochemistry of subduction-related magmatic arcs, with an emphasis on primitive andesite and lower crust. In: Holland, H.D., Turekian, K.K. (Eds.), Treatise on Geochemistry, vol. 3. Elsevier–Pergamon, Oxford, pp. 593–659.

Kelemen, P.B., Yogodzinski, G.M., 2007. High-magnesian andesite from Mount Shasta: a product of magma mixing and contamination, not a primitive melt: comment and reply. Geology 35, 149.

Kelemen, P.B., Hanghøj, K., Greene, A.R., 2014. One view of the geochemistry of subduction-related magmatic arcs, with an emphasis on primitive andesite and lower crust. In: Holland, H.D., Turekian, K.K. (Eds.), Treatise on Geochemistry, vol. 4, second edition. Elsevier, Oxford, pp. 749–806.

Klemme, S., Blundy, J.D., Wood, B.J., 2002. Experimental constraints on major and trace element partitioning during partial melting of eclogite. Geochim. Cosmochim. Acta 66 (17), 3109–3123.

Kylander-Clark, A.R.C., Hacker, B.R., Cottle, J.M., 2013. Laser-ablation split-stream ICP petrochronology. Chem. Geol. 345, 99–112.

Lee, C.-T.A., Lee, T.C., Wu, C.-T., 2014. Modeling the compositional evolution of recharging, evacuating, and fractionating (REFC) magma chambers: implications for differentiation of arc magmas. Geochim. Cosmochim. Acta 143, 8–22.

Macpherson, C.G., Dreher, S.T., Thirlwall, M.F., 2006. Adakites without slab melting: high pressure differentiation of island arc magma, Mindanao, the Philippines. Earth Planet. Sci. Lett. 243 (3–4), 581–593.

Martin, H., 1986. Effect of steeper Archean geothermal gradient on geochemistry of subduction zone magmas. Geology 14, 753–756.

McDonough, W.F., Sun, S.S., 1995. The composition of the Earth. Chem. Geol. 120, 223–253.

Meisel, T., Schoner, N., Paliulionyte, V., Kahr, E., 2002. Determination of rare earth elements, Y, Th, Zr, Hf, Nb and Ta in geological reference materials G-2, G-3, SCo-1 and WGB-1 by sodium peroxide sintering and inductively coupled plasma-mass spectrometry. Geostand. Newsl. 26, 53–61.

Miller, D.M., Goldstein, S.L., Langmuir, C.H., 1994. Cerium lead and lead-isotope ratios in arc magmas and the enrichment of lead in the continents. Nature 368 (6471), 514–520.

Osborn, E.F., 1959. Role of oxygen pressure in the crystallization and differentiation of basaltic magma. Am. J. Sci. 257 (9), 609–647.

Perfit, M.R., Brueckner, H., Lawrence, J.R., Kay, R.W., 1980. Trace element and isotopic variations in a zoned pluton and associated volcanic rocks, Unalaska Island, Alaska: a model for fractionation in the Aleutian calcalkaline suite. Contrib. Mineral. Petrol. 73 (1), 69–87.

Peucker-Ehrenbrink, B., Hofmann, A.W., Hart, S.R., 1994. Hydrothermal lead transfer from mantle to continental crust: the role of metalliferous sediments. Earth Planet. Sci. Lett. 125, 129–142.

Plank, T., Langmuir, C.H., 1993. Tracing trace elements from sediment input to volcanic output at subduction zones. Nature 362, 739–743.

Plank, T., Balzer, V., Carr, M., 2002. Nicaraguan volcanoes record paleoceanographic changes accompanying closure of the Panama gateway. Geology 30, 1087–1090.

Plank, T., 2014. 4.17 – The chemical composition of subducting sediments. In: Holland, H.D., Turekian, K.K. (Eds.), Treatise on Geochemistry, second edition. Elsevier, Oxford, pp. 607–629.

Ringwood, A.E., Green, D.H., 1966. An experimental investigation of the Gabbro-Eclogite transformation and some geophysical implications. Tectonophysics 3 (5), 383–427.

Rioux, M., Mattinson, J., Hacker, B., Kelemen, P.B., Blusztajn, J., Hanghoj, K., Gehrels, G., 2010. Intermediate to felsic middle crust in the accreted Talkeetna arc, the Alaska Peninsula and Kodiak Island, Alaska: an analogue for low-velocity middle crust in modern arcs. Tectonics 29.

Rudnick, R.L., Fountain, D.M., 1995. Nature and composition of the continental-crust – a lower crustal perspective. Rev. Geophys. 33, 267–309.

Rudnick, R.L., Gao, S., 2003. Composition of the continental crust. In: Holland, H.D., Turekian, K.K. (Eds.), Treatise on Geochemistry, vol. 3. Elsevier–Pergamon, Oxford, pp. 1–64.

Ruscitto, D.M., Wallace, P.J., Kent, A.J.R., 2010. Revisiting the compositions and volatile contents of olivine-hosted melt inclusions from the Mount Shasta region: implications for the formation of high-Mg andesites. Contrib. Mineral. Petrol. 162, 109–132.

Salters, V.J.M., Stracke, A., 2004. Composition of the depleted mantle. Geochem. Geophys. Geosyst. 5.

Sarbas, B., 2008. The GEOROC database as part of a growing geoinformatics network. In: Brady, S.R., Sinha, A.K., Gundersen, L.C. (Eds.), Geoinformatics 2008 – Data to Knowledge, Proceedings: U.S. Geological Survey Scientific Investigations Report 2008-5172. USGS, pp. 42–43.

Shillington, D.J., Van Avendonk, H.J.A., Holbrook, W.S., Kelemen, P.B., Hornbach, M.J., 2004. Composition and structure of the central Aleutian island arc from arc-parallel wide-angle seismic data. Geochem. Geophys. Geosyst. 5.

Shimoda, G., Tatsumi, Y., Nohda, S., Ishizaka, K., Jahn, B.M., 1998. Setouchi high-Mg andesites revisited: geochemical evidence for melting of subducting sediments. Earth Planet. Sci. Lett. 160 (3–4), 479–492.

Singer, B.S., Jicha, B.R., Leeman, W.P., Rogers, N.W., Thirlwall, M.F., Ryan, J., Nicolaysen, K.E., 2007. Along-strike trace element and isotopic variation in Aleutian Island arc basalt: subduction melts sediments and dehydrates serpentine. J. Geophys. Res., Solid Earth 112, B6.

Sisson, T.W., Grove, T.L., 1993. Experimental investigations of the role of H_2O in calc-alkaline differentiation and subduction zone magmatism. Contrib. Mineral. Petrol. 113, 143–166.

Skora, S., Blundy, J., 2010. High-pressure hydrous phase relations of radiolarian clay and implications for the involvement of subducted sediment in arc magmatism. J. Petrol. 51, 2211–2243.

Stern, C.R., Kilian, R., 1996. Role of the subducted slab, mantle wedge and continental crust in the generation of adakites from the Andean Austral volcanic zone. Contrib. Mineral. Petrol. 123 (3), 263–281.

Straub, S.M., Gomez-Tuena, A., Stuart, F.M., Zellmer, G.F., Espinasa-Perena, R., Cai, Y., Iizuka, Y., 2011. Formation of hybrid arc andesites beneath thick continental crust. Earth Planet. Sci. Lett. 303, 337–347.

Suyehiro, K., Takahashi, N., Ariie, Y., Yokoi, Y., Hino, R., Shinohara, M., Kanazawa, T., Hirata, N., Tokuyama, H., Taira, A., 1996. Continental crust, crustal underplating, and low-Q upper mantle beneath an oceanic island arc. Science 272 (5260), 390–392.

Tatsumi, Y., 2000. Continental crust formation by delamination in subduction zones and complementary accumulation of the enriched mantle I component in the mantle. Geochem. Geophys. Geosyst. 1, 1–17.

Tatsumi, Y., Shukuno, H., Tani, K., Takahashi, N., Kodaira, S., Kogiso, T., 2008. Structure and growth of the Izu–Bonin–Mariana arc crust: 2. Role of crust–mantle transformation and the transparent Moho in arc crust evolution. J. Geophys. Res., Solid Earth 113 (B2).

Taylor, S.R., McLennan, S.M., 1995. The geochemical evolution of the continental crust. Rev. Geophys. 33 (2), 241–265.

Vervoort, J.D., Plank, T., Prytulak, J., 2011. The Hf–Nd isotopic composition of marine sediments. Geochim. Cosmochim. Acta 75, 5903–5926.

Yogodzinski, G.M., Rubenstone, J.L., Kay, S.M., Kay, R.W., 1993. Magmatic and tectonic development of the western Aleutians: an oceanic arc in a strike-slip setting. J. Geophys. Res. 98 (B7), 11807.

Yogodzinski, G.M., Volynets, O.N., Koloskov, A.V., Seliverstov, N.I., Matvenkov, V.V., 1994. Magnesian andesites and the subduction component in a strongly calc-alkaline series at Piip Volcano, Far Western Aleutians. J. Petrol. 35, 163–204.

Yogodzinski, G.M., Kay, R.W., Volynets, O.N., Koloskov, A.V., Kay, S.M., 1995. Magnesian Andesite in the Western Aleutian Komandorsky Region – implications for slab melting and processes in the mantle wedge. Geol. Soc. Am. Bull. 107 (5), 505–519.

Yogodzinski, G.M., Kelemen, P.B., 1998. Slab melting in the Aleutians: implications of an ion probe study of clinopyroxene in primitive adakite and basalt. Earth Planet. Sci. Lett. 158 (1–2), 53–65.

Yogodzinski, G.M., Lees, J.M., Churikova, T.G., Dorendorf, F., Woerner, G., Volynets, O.N., 2001. Geochemical evidence for the melting of subducting oceanic lithosphere at plate edges. Nature 409 (6819), 500–504.

Yogodzinski, G.M., Kelemen, P.B., 2007. Trace elements in clinopyroxenes from Aleutian xenoliths: implications for primitive subduction magmatism in an island arc. Earth Planet. Sci. Lett. 256, 617–632.

Yogodzinski, G.M., Vervoort, J.D., Brown, S.T., Gerseny, M., 2010. Subduction controls of Hf and Nd isotopes in lavas of the Aleutian island arc. Earth Planet. Sci. Lett. 300 (3–4), 226–238.

Yogodzinski, G.M., Brown, S.T., Kelemen, P.B., Vervoort, J.D., Portnyagin, M., Sims, K.W.W., Hoernle, K., Jicha, B.R., Werner, R., 2015. The role of subducted basalt in the source of island arc magmas: evidence from seafloor lavas of the western Aleutians. J. Petrol. 56, 441–492.

Zimmer, M.M., Plank, T., Hauri, E.H., Yogodzinski, G.M., Stelling, P., Larsen, J., Singer, B., Jicha, B., Mandeville, C., Nye, C.J., 2010. The role of water in generating the Calc-alkaline trend: new volatile data for Aleutian magmas and a new Tholeiitic Index. J. Petrol. 51 (12), 2411–2444.

Distinctly different parental magmas for plutons and lavas in the central Aleutian arc

Yue Cai[1*], Matthew Rioux[2], Peter B. Kelemen[1,3], Steven L. Goldstein[1,3], Louise Bolge[1], Andrew R. C. Kylander-Clark[4]

[1]Lamont-Doherty Earth Observatory of Columbia University, 61 Rt. 9W, Palisades, NY 10964, USA

[2] Earth Research Institute, University of California, Santa Barbara, CA, 93106, USA

[3] Department of Earth and Environmental Sciences, Columbia University, 61 Rt. 9W, Palisades, NY 10964, USA

[4] Department of Earth Science, University of California, Santa Barbara, CA, 93106

Supplementary Materials

1. U-Pb zircon geochronology

Method:

U-Pb zircon geochronology of the plutonic samples was carried out by laser ablation-inductively coupled plasma-mass spectrometry (LA-ICP-MS) at the University of California, Santa Barbara. Zircons were mounted in epoxy, polished to expose grain cores and imaged by cathodoluminescence prior to analysis. LA-ICP-MS analyses followed the procedures outlined in Kylander-Clark et al. (2013). A 2% uncertainty was added in quadrature to the $^{206}Pb/^{238}U$, $^{207}Pb/^{235}U$ and $^{207}Pb/^{206}Pb$ analytical uncertainties to account for observed internal variability in excess of counting statistics of standard analyses in the UCSB lab. $^{206}Pb/^{238}U$ dates were corrected for initial ^{230}Th exclusion from the ^{238}U decay chain based on the measured Th/U of the zircon and an assumed Th/U of the melt of 2.7. The Th/U of the melt was estimated from whole rock ICP-MS Th/U of the dated samples, which range from 1.9–3.5, with a mean of 2.7. Large variations (± 1) in the assumed Th/U of the melt lead to relatively small changes in the Th-corrected $^{206}Pb/^{238}U$ dates (< +0.03/-0.06 Ma for most spot dates), and the propagated uncertainties in the assumed Th/U of the melt are overwhelmed by the analytical uncertainties, which are typically an order of magnitude larger. Data were common Pb corrected using a ^{207}Pb correction assuming a common Pb

$^{207}Pb/^{206}Pb = 0.83$. $^{206}Pb/^{204}Pb$ ratios for the analyses are reported in Table S2, however, the ratios are likely inaccurate due to low ^{204}Pb count rates and uncorrected ^{204}Hg interferences, making a ^{207}Pb common Pb correction more accurate. Concordia plots, weighted mean plots and and weighted mean calculations were generated using the U-Pb_Redux software package (Bowring et al., 2011; McLean et al., 2011).

Data interpretation:

The fractionation corrected U-Pb data for each sample typically consist of a cluster of concordant or nearly concordant data points and a variable number of more discordant analyses (Tera-Wasserburg concordia diagrams, Figure S1). The discordant analyses are attributed to mixing between radiogenic Pb from the zircon and a common Pb component; common-Pb corrected $^{206}Pb/^{238}U$ dates for these data points generally agree with the $^{206}Pb/^{238}U$ dates of the more concordant analyses (Table S2). To minimize the uncertainty introduced by the common-Pb correction, spot analyses that were >15% discordant were excluded from the weighted mean calculations.

The concordant and near concordant (<15% discordant) spot analyses generally form a single cluster of data on the concordia diagrams. The mean square of the weighted deviates (MSWD) or reduced chi-squared statistic of the weighted mean Th and common Pb corrected $^{206}Pb/^{238}U$ dates are higher than expected for repeat analyses of a single age for most samples (i.e. MSWD >> 1; two-sided p-value for the chi-squared goodness of fit ≤0.05; Table S2 'weighted mean all'). The elevated MSWD or apparent variability in the data may reflect: 1. Underestimation of the analytical uncertainties on the spot analyses; 2. True variability in the zircon $^{206}Pb/^{238}U$ ages due to protracted zircon crystallization; 3. Minor Pb-loss leading to anomalously young dates for some spots; or 4. Inheritance of slightly older zircons leading to older dates for some spots. It is not possible to differentiate between these scenarios based on the current dataset. However, we feel the data topology is most consistent with the interpretation that the slightly younger and older spots reflect minor Pb loss and inheritance, respectively.

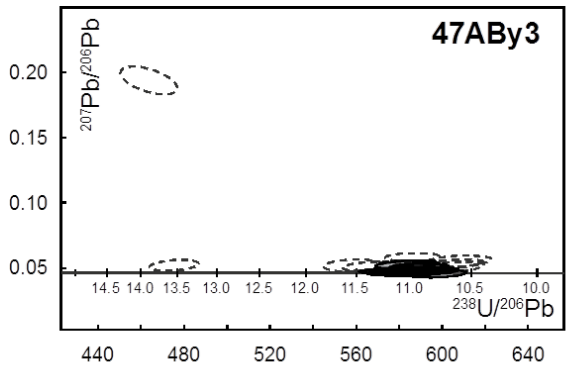
47ABy3
$^{207}Pb/^{206}Pb$
$^{238}U/^{206}Pb$

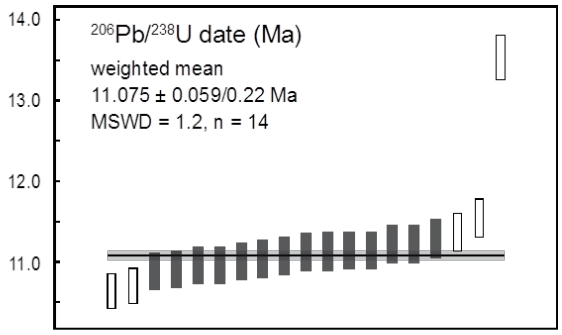
$^{206}Pb/^{238}U$ date (Ma)
weighted mean
11.075 ± 0.059/0.22 Ma
MSWD = 1.2, n = 14

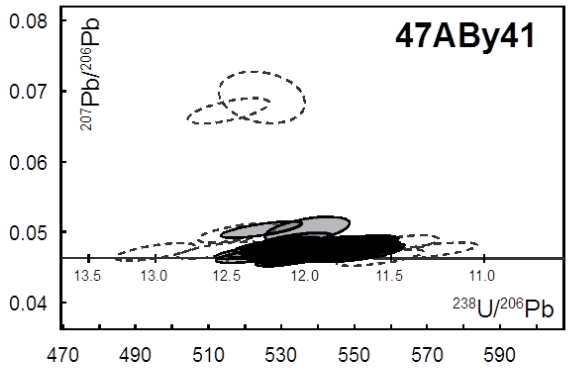
47ABy41
$^{207}Pb/^{206}Pb$
$^{238}U/^{206}Pb$

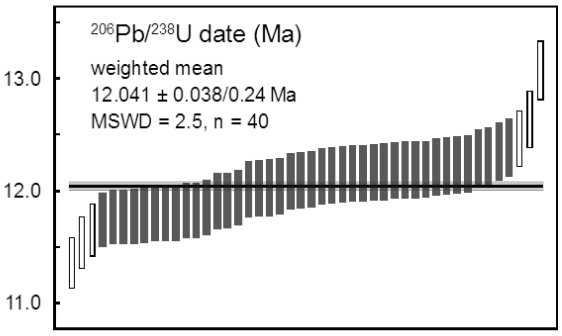
$^{206}Pb/^{238}U$ date (Ma)
weighted mean
12.041 ± 0.038/0.24 Ma
MSWD = 2.5, n = 40

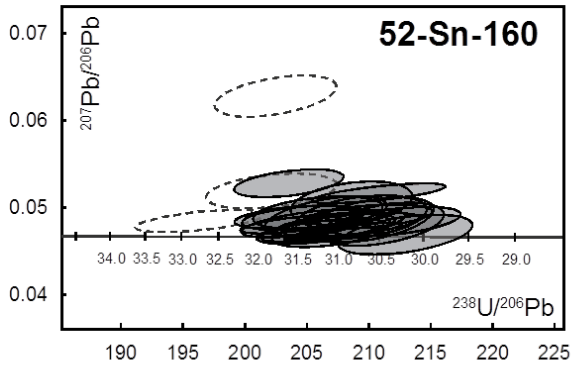
52-Sn-160
$^{207}Pb/^{206}Pb$
$^{238}U/^{206}Pb$

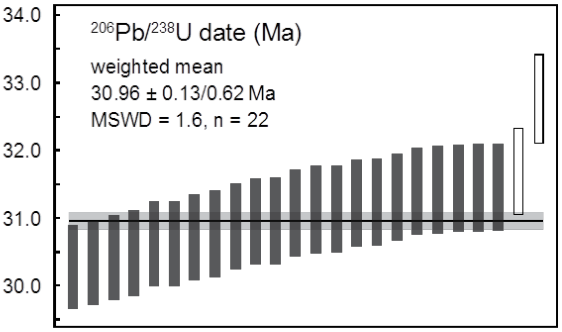
$^{206}Pb/^{238}U$ date (Ma)
weighted mean
30.96 ± 0.13/0.62 Ma
MSWD = 1.6, n = 22

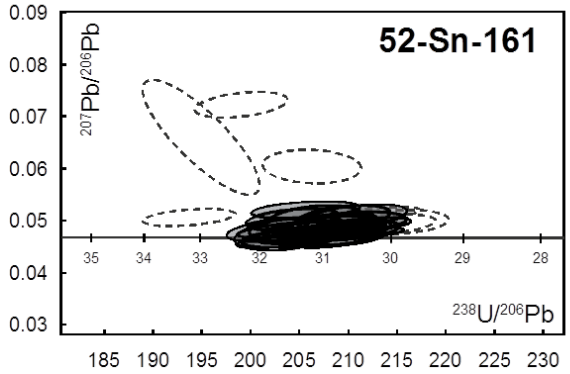
52-Sn-161
$^{207}Pb/^{206}Pb$
$^{238}U/^{206}Pb$

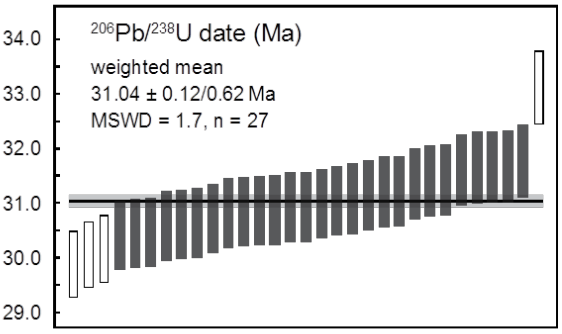
$^{206}Pb/^{238}U$ date (Ma)
weighted mean
31.04 ± 0.12/0.62 Ma
MSWD = 1.7, n = 27

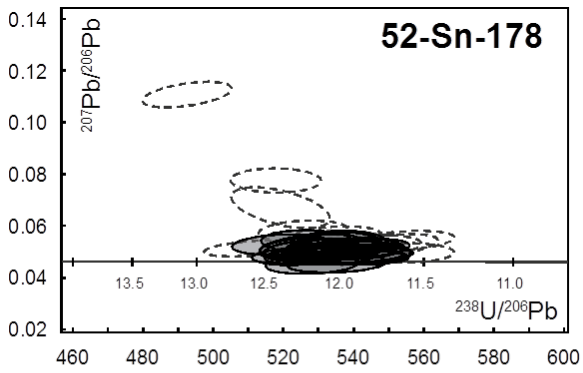
52-Sn-178
$^{207}Pb/^{206}Pb$
$^{238}U/^{206}Pb$

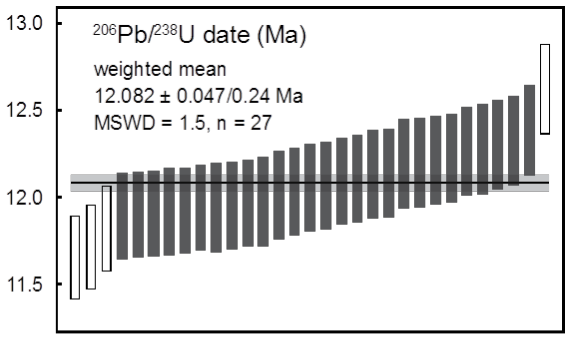
$^{206}Pb/^{238}U$ date (Ma)
weighted mean
12.082 ± 0.047/0.24 Ma
MSWD = 1.5, n = 27

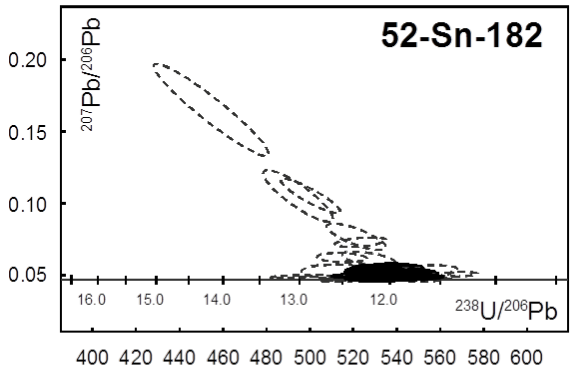
52-Sn-182
$^{207}Pb/^{206}Pb$
$^{238}U/^{206}Pb$

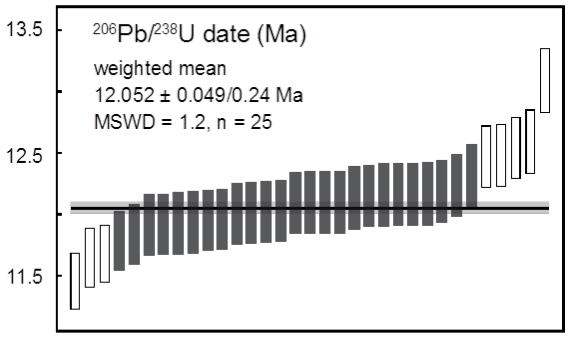
$^{206}Pb/^{238}U$ date (Ma)
weighted mean
12.052 ± 0.049/0.24 Ma
MSWD = 1.2, n = 25

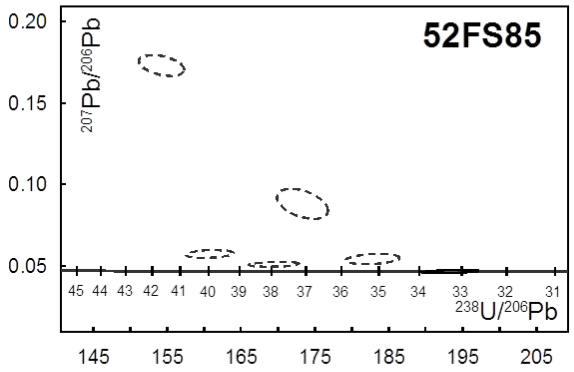
52FS85
$^{207}Pb/^{206}Pb$
$^{238}U/^{206}Pb$

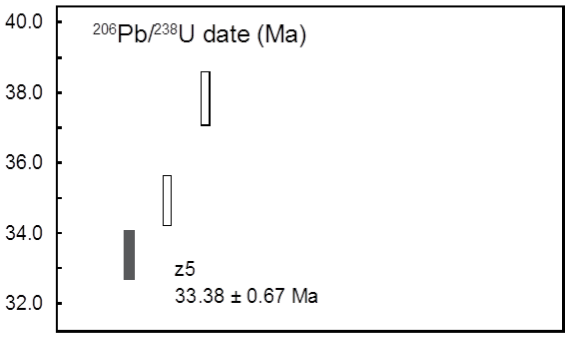
$^{206}Pb/^{238}U$ date (Ma)
z5
33.38 ± 0.67 Ma

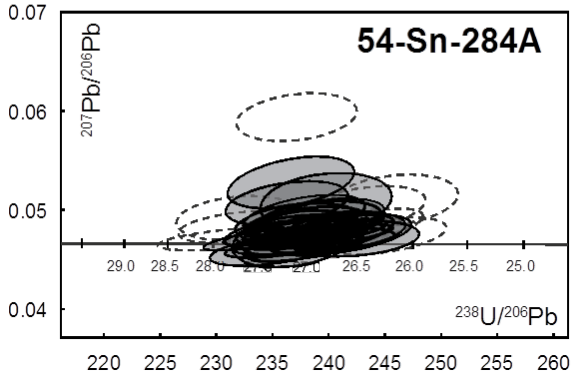
54-Sn-284A
$^{207}Pb/^{206}Pb$
$^{238}U/^{206}Pb$

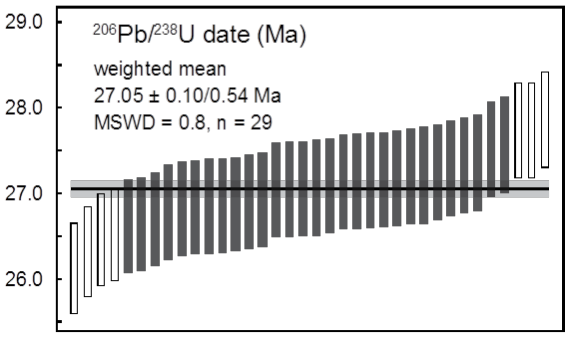
$^{206}Pb/^{238}U$ date (Ma)
weighted mean
27.05 ± 0.10/0.54 Ma
MSWD = 0.8, n = 29

52

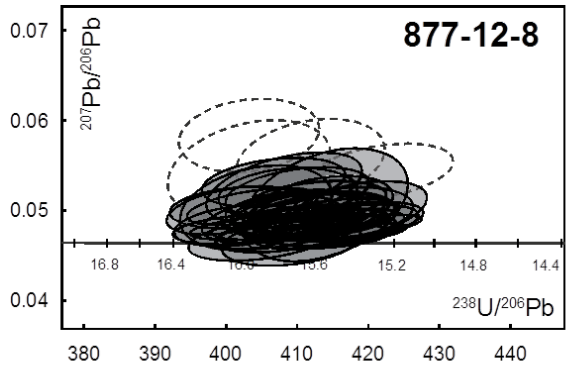
877-12-8
$^{207}Pb/^{206}Pb$
$^{238}U/^{206}Pb$

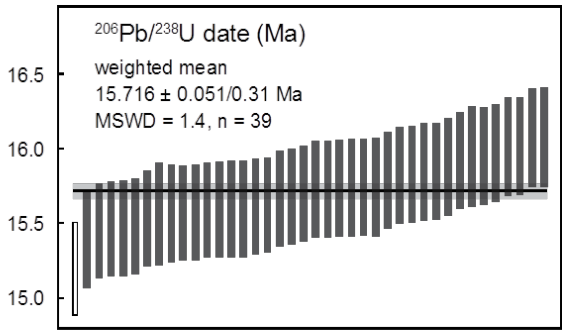
$^{206}Pb/^{238}U$ date (Ma)
weighted mean
15.716 ± 0.051/0.31 Ma
MSWD = 1.4, n = 39

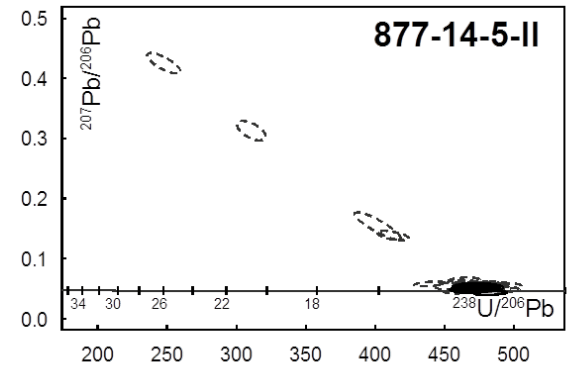
877-14-5-II
$^{207}Pb/^{206}Pb$
$^{238}U/^{206}Pb$

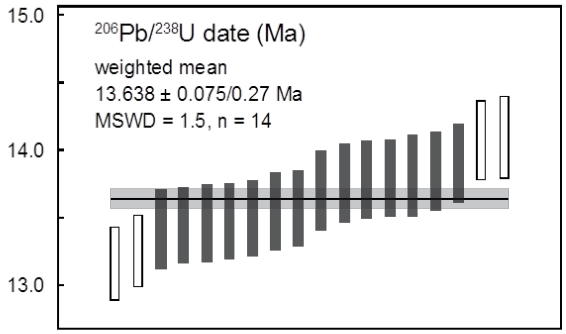
$^{206}Pb/^{238}U$ date (Ma)
weighted mean
13.638 ± 0.075/0.27 Ma
MSWD = 1.5, n = 14

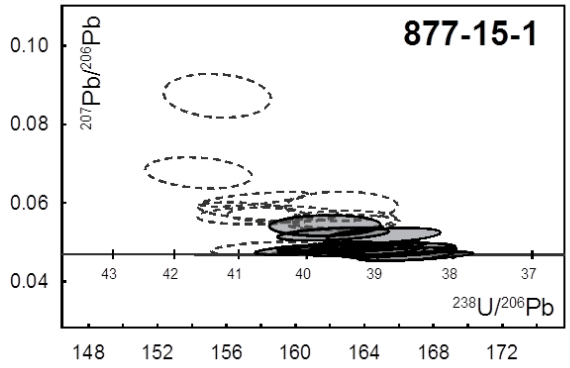
877-15-1
$^{207}Pb/^{206}Pb$
$^{238}U/^{206}Pb$

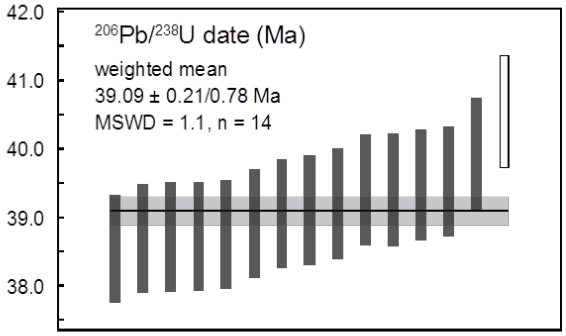
$^{206}Pb/^{238}U$ date (Ma)
weighted mean
39.09 ± 0.21/0.78 Ma
MSWD = 1.1, n = 14

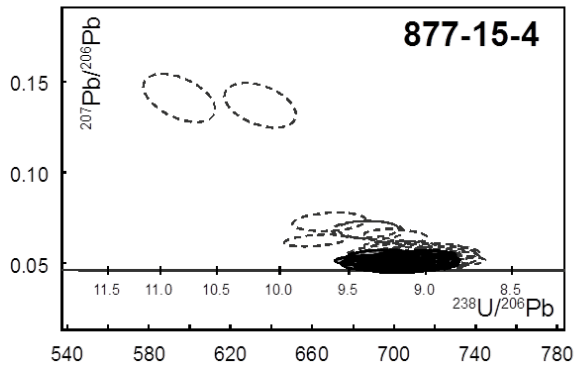
877-15-4
$^{207}Pb/^{206}Pb$
$^{238}U/^{206}Pb$

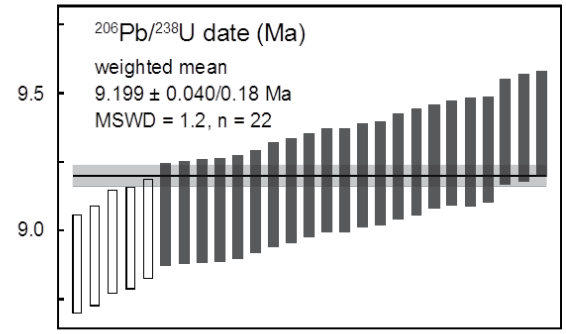
$^{206}Pb/^{238}U$ date (Ma)
weighted mean
9.199 ± 0.040/0.18 Ma
MSWD = 1.2, n = 22

Fig. S1. *Tera-Wasserburg concordia and weighted mean plots for each sample. The concordia plots include all data from each sample and the plotted data are not ^{230}Th or common Pb corrected; data excluded from the weighted mean calculations are plotted as dashed ellipses. Weighted mean plots are ^{230}Th and common Pb corrected $^{206}Pb/^{238}U$ dates and exclude dates that are >15% discordant. Data included in the weighted mean calculations are solid bars and excluded near-concordant (<15% discordant) data are open bars. Uncertainties on the weighted mean dates are reported as ±internal uncertainties/external uncertainties Ages along concordia are in Ma.*

The weighted mean plots in Figure S1 show weighted mean $^{206}Pb/^{238}U$ dates calculated excluding the anomalously old and young analyses. These dates are reported as 'wtd mn preferred' in Table S2. The culled datasets generally have reduced chi-squared statistics for the number of analyzed spots consistent with repeat analyses of a single age population (i.e. MSWD ~ 1; two-sided p-value for the chi-squared goodness of fit >0.05), with the exception of samples 47ABy41 and 52-Sn-161 which still have slightly higher MSWD (2.5 and 1.7, respectively). Uncertainties on the weighted mean dates in Figure S1 and Table S2 are reported as ±internal uncertainties/external uncertainties; external uncertainties are set at 2% based on the long term reproducibility of zircon standard analyses for the UCSB lab. The final weighted mean dates are relatively insensitive to the exact data interpretation; the culled weighted mean dates and the weighted mean dates for the full date set for each sample overlap within uncertainty, with differences of <0.1 Ma. Sample 52FS85 only yielded 6 zircons, which gave variable dates. We interpret the Th and common Pb corrected $^{206}Pb/^{238}U$ of the youngest concordant spot analysis as the best estimate of the crystallization age of this sample.

2. Whole rock major and trace element analyses

Major and trace element analyses were carried out at Lamont-Doherty Earth Observatory (LDEO). Major element analyses were carried out using an Agilent ICP-OES on rock powders digested with $Li_2B_4O_7$ flux fusion. Trace element analyses were carried out on a VG PlasmaQuad ExCell quadrupole ICP-MS. In order to ensure complete digestion of zircons and other accessory phases for trace element analyses, we conducted both traditional hotplate HNO_3-HF acid digestion and Na_2O_2 sintering for the trace elements, following procedures of Meisel et al. (2002). For sintered digestions, 100mg of rock powder was mixed with 500mg of Na_2O_2 (Fluka®, purum) in glassy carbon crucibles and heated to 490°C

82 in a muffle furnace for 30 minutes. After cooling, ultrapure water (Milli-Q) was added drop-wise to the
83 sintered cake which triggers a vigorous reaction where metal peroxides react with water to form metal
84 hydroxides. Acid cleaned watch glasses were used to cover each crucible in order to prevent sample loss
85 and cross contamination from splashing during the reaction. After the reaction subsides, 5ml of 3N HNO_3
86 acid is added to the hydroxide-water mixture which completely dissolves the sample and forms a clear
87 solution. Both the watch glass and the crucibles are carefully rinsed 3 times with 3N HNO_3 using pipettes
88 to recover all the samples. Finally, the fully dissolved samples are transferred to acid cleaned bottles for
89 further dilution and the diluted sample solutions in 3% HNO_3 were measured directly on the quadrupole
90 ICP-MS. In order to minimize biases introduced by sample matrix, a mixed rinse solution of 0.1% Na_2O_2
91 and 3% HNO_3 was used during the measurements of the sintered samples. For both major and trace
92 element analyses, a drift solution made with mixed sample solutions was analyzed at the start and end of
93 each run period and after every five unknowns to monitor instrumental drift. After drift correction,
94 procedural blanks were measured and subtracted from the raw counts of the standards and the unknown
95 samples. The blank correction is generally <1% for both digestion methods. Data reported are corrected
96 against USGS standards using GeoRem recommended values (Table S1).
97 Except for Zr and Hf, trace element data from both hotplate and sintered digestion methods agree
98 with each other within 6%. Hf and Zr contents of the sintered digestions are variably higher (1.2 to 12.1
99 times) than those from the hotplate digestion. This is likely due to incomplete digestion of zircon crystals
100 in hotplate digestions, which are completely digested through Na_2O_2 sintering. Concentrations of the
101 heavy-rare-earth-elements (HREE) are also slightly higher in the sintered digestions, which also likely
102 reflect incomplete digestion of minor mineral phases, such as zircons, in hotplate digestions. For these
103 reasons, in order to better compare with literature data and maintain consistency in calculating elemental
104 ratios, we use only the sintered data for La, Nd, Sm, Eu, Pr, Tb, Gd, Dy, Yb, Lu, Y, Zr, Hf (Table S1, Fig.
105 S2).

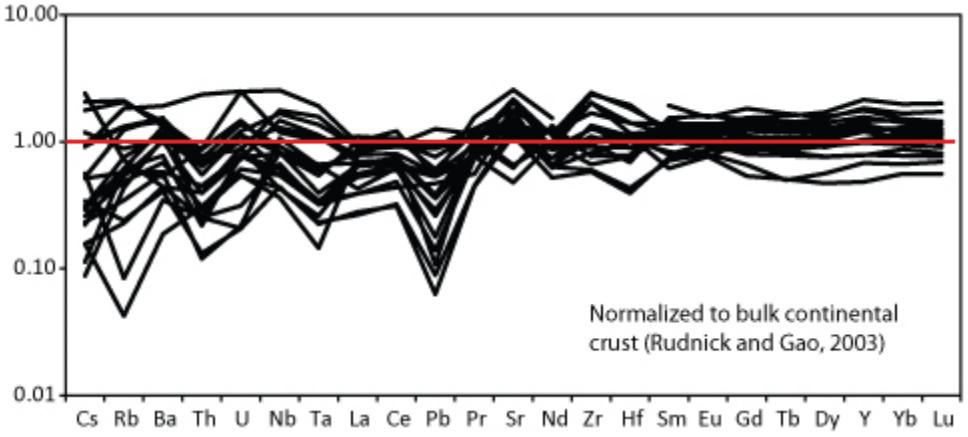

Fig. S2. *Trace element contents normalized to bulk continental crust (Rudnick and Gao, 2003).*

3. Literature data sorting and fractionation correction

To calculate the average central Aleutian lava composition for Figure 1, trace element data measured by XRF or before the 1980's were removed from the database to maintain consistency in data quality. Th data from Brophy et al. (1990) are removed from the database as they appear systematically higher than similar samples reported in more recent studies. Dy* and Tb* are calculated for samples missing Tb or Dy data using the available Dy and Tb data from central Aleutian lavas, which are highly correlated and yield the following relationship: $Dy=6.3932\times Tb - 0.0837$; $Tb = 0.1539\times Dy + 0.0244$ ($r = 0.99$, $n = 260$). In Figures 2 and 3, literature $^{143}Nd/^{144}Nd$ data with known Nd standard information were re-normalized to La Jolla value of 0.511858 to better compare with our new data.

Trace element data are corrected for fractional crystallization to Mg# of 0.5 by regressing the natural log of trace element concentrations to molar Mg#, where Mg# = molar MgO/(MgO+FeO*), using literature data for central Aleutian lavas, following the method of Behn et al., (2011). The regression would follow $[TE] = A\times e^{(B*Mg\#)}$. Fractionation corrected trace element concentrations are calculated as $[TE]_{0.5} = [TE] \times e^{(B*(0.5-Mg\#))}$.

4. Whole rock isotopic analyses (Pb-Nd-Sr-Hf)

Pb-Nd-Sr-Hf isotope analyses were conducted at LDEO. Samples were first leached in 6N HCl at 100°C for 30 minutes and sonicated in 6N HCl for 30 minutes, then sonicated and leached with Milli-Q water three times before hotplate digestion. The samples were then digested with a HNO_3-HF acid

mixture @120°C on a hotplate for column chemistry. For Hf isotope analyses, a subset of unleached samples was also sintered following procedures of Kleinhanns et al. (2002). Similar to the procedure for trace element digestion, Milli-Q water was added drop-wise to the sintered cake. However, instead of adding acids directly to this mixture, the samples are first transferred into 15ml centrifuge tubes and centrifuged to remove the supernatant that contains dissolved Na and Si as Na_2SiO_4. After the supernatant was pipetted off and discarded, the hydroxide precipitates were mixed thoroughly with Milli-Q water and centrifuged again to further remove the Na and Si by removing the supernatant. After three such Milli-Q water rinses, the hydroxide precipitates were fully dissolved in 6N HCl and transferred to acid cleaned Teflon® vials for routine column chemistry. Pb was extracted using Bio-rad AG®1-X8 resin and HBr and HCl column chromatography. Nd was extracted using Tru-Spec® resin followed by Eichrom Ln-Spec® resin and HNO_3. Sr was extracted using Eichrom Sr-Spec® resin. Hf was extracted using Eichrom Ln-Spec® resin (Münker et al., 2001). The total procedural blanks for Pb in hotplate digestions range from 21-30 pg and the blanks for Nd, Hf and Sr are negligible.

Nd, Pb, Hf, and Sr isotopes were measured on a ThermoScientific Neptune Plus multi-collector MC-ICP-MS in static mode; some Sr isotope ratios were measured on a VG-Sector 54 TIMS in multi-dynamic mode (Table S1). The MC-ICP-MS instrumental drift is monitored by standard-sample bracketing using JNdi-1 for Nd, a Johnson-Matthey lab Hf standard with Hf isotope ratios indistinguishable from JMC 475, NBS 987 Sr, and NBS 981 Pb. Typically 30-70 standards and 20-30 samples are analyzed during a 24-hour long run period, and reported 2SD external errors reflect the reproducibility of the standards. Reported values are corrected to those of the international standards. Quality control was further evaluated through measurements of the La Jolla Nd solution standard, and rock standards BCR-2 and BHVO-2. The analytical metadata (standards data, amounts per sample, signal intensities, values used for international standards, results, and reproducibility) are listed in Table S5.

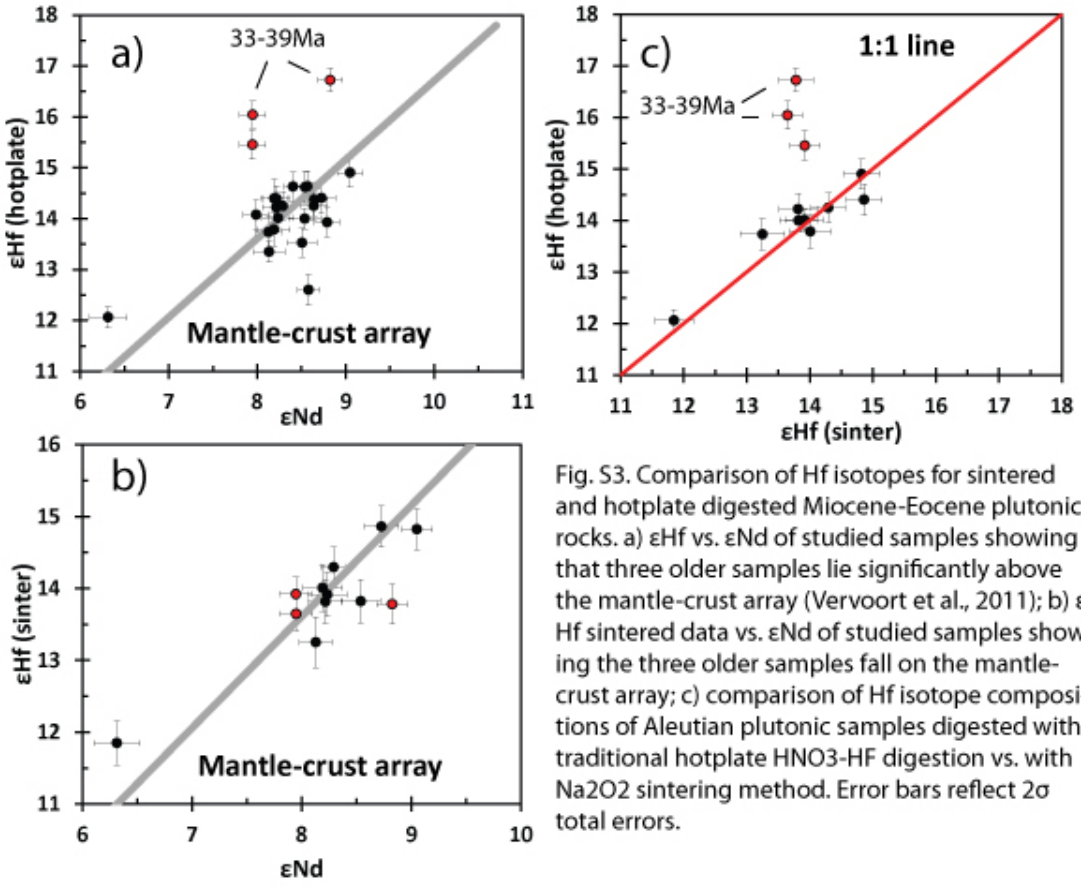

Fig. S3. Comparison of Hf isotopes for sintered and hotplate digested Miocene-Eocene plutonic rocks. a) εHf vs. εNd of studied samples showing that three older samples lie significantly above the mantle-crust array (Vervoort et al., 2011); b) ε Hf sintered data vs. εNd of studied samples showing the three older samples fall on the mantle-crust array; c) comparison of Hf isotope compositions of Aleutian plutonic samples digested with traditional hotplate HNO3-HF digestion vs. with Na2O2 sintering method. Error bars reflect 2σ total errors.

In εNd-εHf isotope space (present-day), three older samples (33-39Ma) dissolved without sintering plot significantly above the Nd-Hf mantle-crust array (Fig. S3a). However, after sintered digestion these samples have significantly lower εHf (by 1.5 to 2.9 epsilon units) and fall on the array (Fig. S3b). These observations indicate that without sintering some zircons with high Hf concentrations were incompletely digested. Measured Hf concentrations of zircon-bearing samples from the hotplate digestions are generally less than 20% of the sintered digestions (Table S3). Moreover, the hotplate digestions have much higher Lu/Hf ratios (e.g., 0.51 and from hotplate digestions *vs.* 0.11 from sintered digestions), reflecting high Lu/Hf in the rock matrix and very low Lu/Hf in the zircons.

Such differences in parent/daughter ratios can generate significant differences between Hf isotope ratios in the matrix and the zircons, on the order of a few εHf units over some tens of millions of years.

The anomalously high Hf isotope ratios from hotplate digested samples thus appear to mainly reflect the composition of the rock matrix, which have high Lu/Hf ratios compared to the bulk sample, and which is readily dissolved during hotplate digestion; while the zircons in some samples, with low Lu/Hf and high Hf contents, remain intact during hotplate digestions. Nevertheless, most samples show minimal difference in εHf values between the two digestion methods, with an average difference of 0.24 or 24ppm (n=9), which is comparable to the analytical error (Fig. S3c).

5. Age correction for isotope ratios

The rocks in this study have ages of up to ~39 Ma, and in order to ensure that our conclusions are not related to post-emplacement radioactive decay, we have evaluated the effect of age (Fig. S4, S5). We calculated initial Nd and Pb isotope ratios of the plutonic samples using their U-Pb zircon ages, and their measured whole-rock parent/daughter element ratios. From these initial ratios, we also calculated what the isotope ratios would be in the present-day mantle source (Figs. S4-S5). For the mantle source evolution since the plutons formed, we used Sm/Nd=0.38, Rb/Sr = 0.01, U/Pb = 0.2, Th/Pb = 0.6 ($^{147}Sm/^{144}Nd$ = 0.1929, $^{87}Rb/^{86}Sr$ = 0.029, $^{238}U/^{204}Pb$ = 12.35, $^{232}Th/^{204}Pb$= 38.24) for the ***DMM*** (***D***epleted ***M***ORB ***M***antle, e.g., Salters and Stracke, 2004) and Sm/Nd=0.32, Rb/Sr = 0.03, U/Pb = 0.14, Th/Pb = 0.53 ($^{147}Sm/^{144}Nd$ = 0.2290, $^{87}Rb/^{86}Sr$ = 0.087, $^{238}U/^{204}Pb$ = 8.642, $^{232}Th/^{204}Pb$= 33.78) for ***PM*** (***P***rimitive ***M***antle, McDonough and Sun, 1995). The age-corrected Nd and Pb isotope data show the same relationships as the present-day isotope ratios – plutonic rocks from the central and eastern Aleutians show overall higher Nd ratios and lower Pb isotope ratios than lavas from the same region, instead they are more similar to lavas from the western Aleutians (Figs. 2-3).

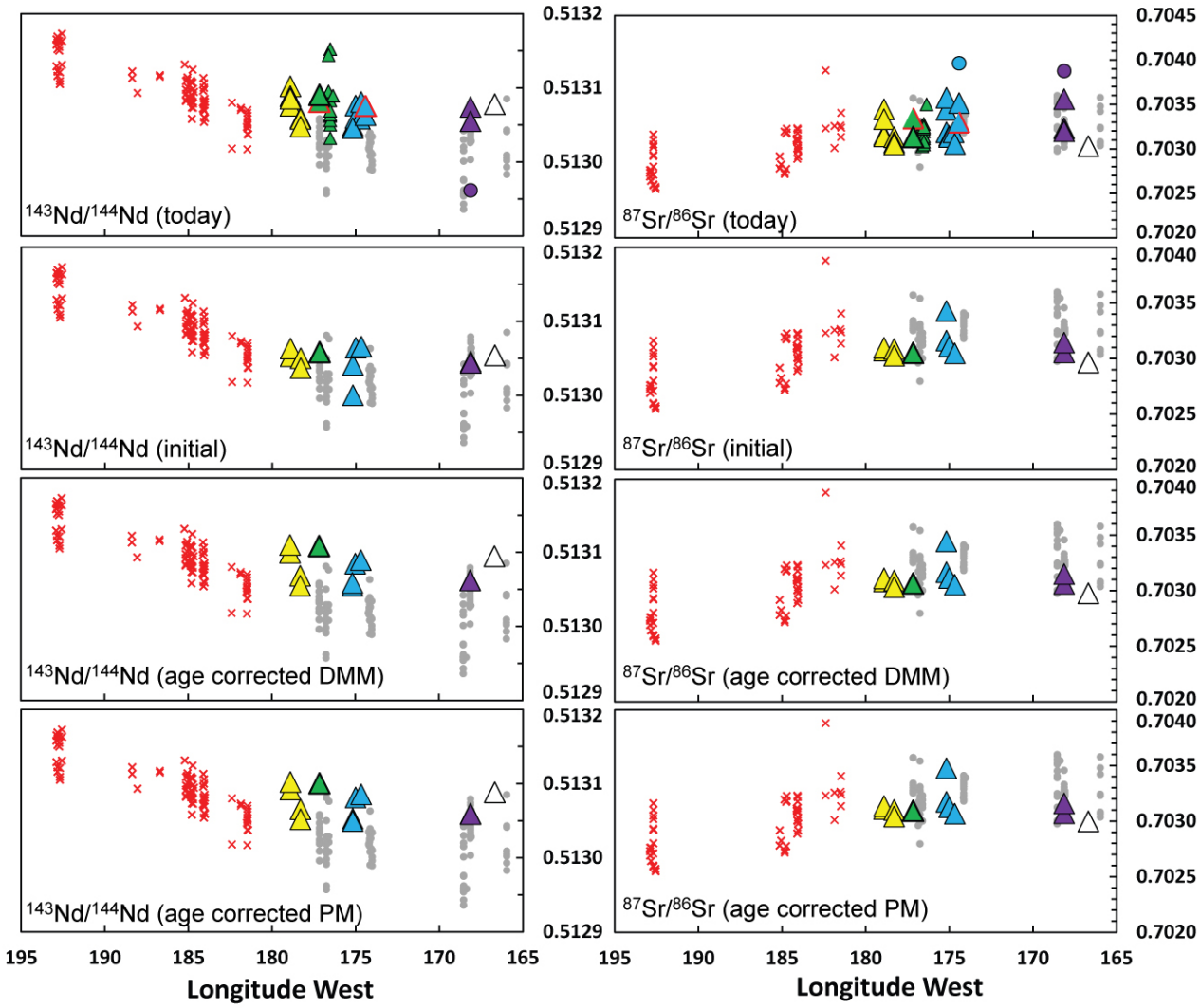

Fig. S4. *Measured and age-corrected data Nd and Sr isotope ratios of Aleutian plutons. The reasons for the age corrections, are explained in the text. All cases show the same relationships between the plutons and the volcanics - plutonic rocks from the central Aleutians show overall higher Nd ratios and lower Pb isotope ratios than lavas from the same region, instead they are more similar to lavas from the western Aleutians.*

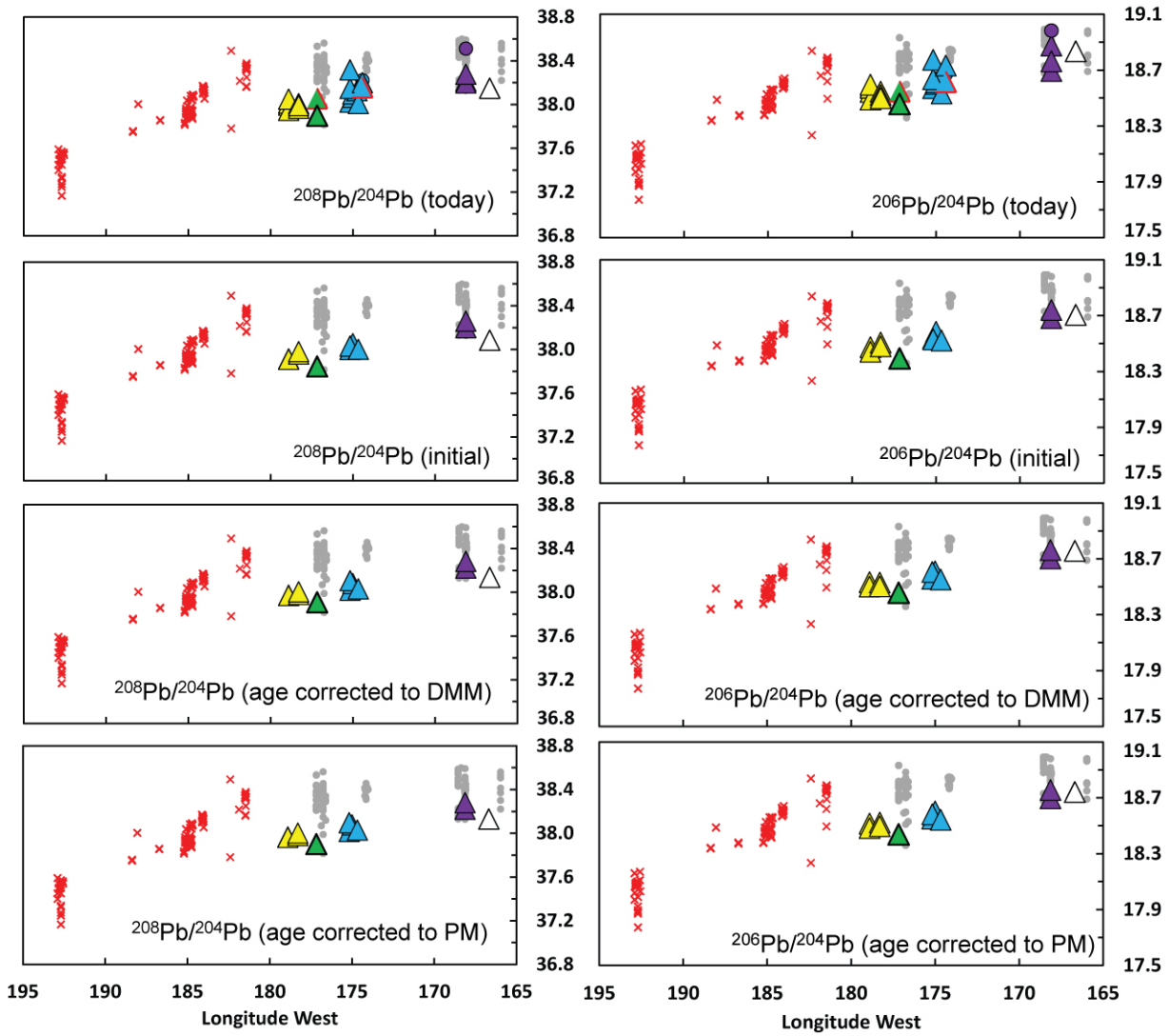

Fig. S5. *Measured and age-corrected data Pb isotope ratios of Aleutian plutons. The reasons for the age corrections, and the approaches, are explained in the text. All cases show the same relationships between the plutons and the volcanics.*

6. Additional figures

Calc-alkaline magmas, including central-eastern Aleutian plutons and western Aleutian lavas, plot in an area subparallel to the tholeiitic lavas from central-eastern Aleutians in MgO vs. Mg# space (Fig. S6 A), with lower MgO at a given Mg# in the calc-alkaline suite. This suggests that the parental magmas of the calc-alkaline magmas and the plutons are cooler than those of the tholeiitic central-eastern Aleutian volcanics. In addition, εNd values of the plutons remain high across a wide range of SiO_2 and MgO contents and they show no correlation with fractionation indices (Fig. S6 B-C). This suggests that (a) the

parental magmas have similar isotope signatures, more depleted than volcanics from the same region, and (b) the differences between the plutons and the volcanics from central-eastern Aleutians are not caused by magma mixing or fractionation.

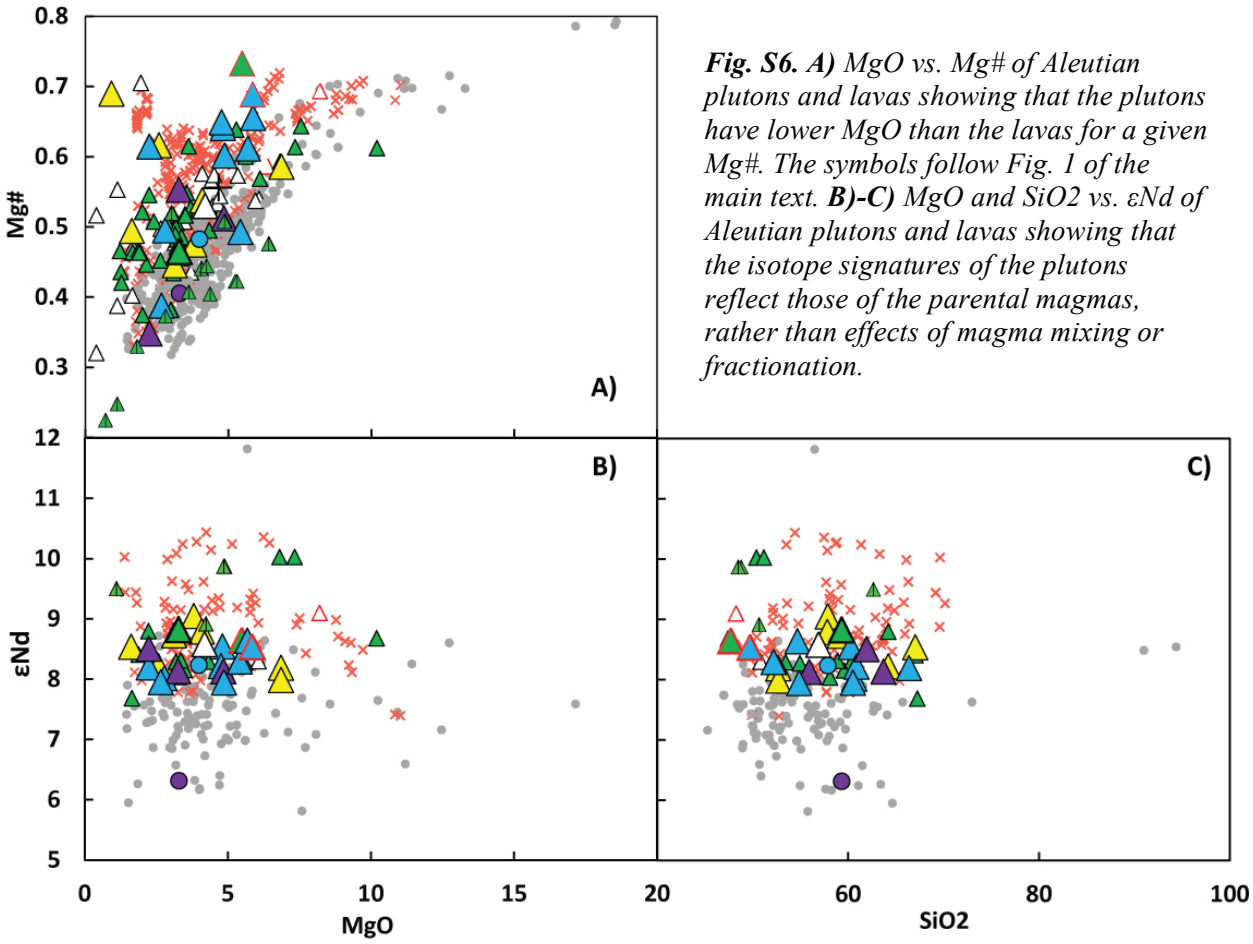

Fig. S6. A) *MgO vs. Mg# of Aleutian plutons and lavas showing that the plutons have lower MgO than the lavas for a given Mg#. The symbols follow Fig. 1 of the main text.* ***B)-C)*** *MgO and SiO2 vs. εNd of Aleutian plutons and lavas showing that the isotope signatures of the plutons reflect those of the parental magmas, rather than effects of magma mixing or fractionation.*

7. References for the Supplementary material:

1. Behn, M. D., Kelemen, P. B., Hirth, G., Hacker, B. R. & Massonne, H.-J. Diapirs as the source of the sediment signature in arc lavas. *Nature Geosci.* **4**, 641-646 (2011)
2. Bouvier, A., Vervoort, J. D. & Patchett, P. J. The Lu-Hf and Sm-Nd isotopic composition of CHUR: Constraints from unequilibrated chondrites and implications for the bulk composition of terrestrial planets. *Earth Planet. Sci. Lett.* **273**, 48-57 (2008).
3. Bowring, J.F., McLean, N.M. & Bowring, S.A., Engineering cyber infrastructure for U-Pb geochronology: Tripoli and U-Pb_Redux. *Geochem. Geophys., Geosyst.* **12**, Q0AA19 (2011)
4. DePaolo, D. J., 1981, Trace element and isotopic effects of combined wallrock assimilation and fractional crystallization: Earth and Planetary Science Letters, v. 53, no. 2, p. 189-202.

5. Gale, A., Dalton, C. A., Langmuir, C. H., Su, Y. & Schilling, J.-G. The mean composition of ocean ridge basalts. *Geochem. Geophys. Geosyst.* **14**, 489-518 (2013).
6. Jacobsen, S. B. & Wasserburg, G. J. Sm-Nd isotopic evolution of Chondrites. *Earth Planet. Sci. Lett.* **50**, 139-155 (1980).
7. Jaffey, A. H., Flynn, K. F., Glendenin, L. E., Bentley, W. C. & Essling, A. M. Precision measurement of the half-lives and specific activities of U235 and U238. *Phys. Rev.* **C4**, 1889-907 (1971).
8. Johnson, M. C. & Plank, T. Dehydration and melting experiments constrain the fate of subducted sediments. *Geochem., Geophys., Geosyst.* **1**, doi:10.1029/1999gc000014 (1999).
9. Kleinhanns, I. C. et al. Combined chemical separation of Lu, Hf, Sm, Nd, and REEs from a single rock digest: Precise and accurate isotope Determinations of Lu-Hf and Sm-Nd using multicollector-ICPMS. *Anal. Chem.* **74**, 67-73 (2002).
10. Kylander-Clark, A. R. C., Hacker, B. R. & Cottle, J. M. Laser-ablation split-stream ICP petrochronology. *Chem. Geol.* **345**, 99-112 (2013).
11. Lugmair, G.W. and Marti, K. Lunar initial 143Nd/144Nd: differential evolution of the lunar crust and mantle. *Earth Planet. Sci. Lett.* **39**, 349-57 (1978).
12. Meisel, T., Schoner, N., Paliulionyte, V. & Kahr, E. Determination of rare earth elements, Y, Th, Zr, Hf, Nb and Ta in geological reference materials G-2, G-3, SCo-1 and WGB-1 by sodium peroxide sintering and inductively coupled plasma-mass spectrometry. *Geost. News. - J. Geost. Geoanal.* **26**, 53-61 (2002).
13. McDonough, W. F. & Sun, S. s. The composition of the Earth. *Chem. Geo.* **120**, 223-253 (1995).
14. McLean, N.M., Bowring, J.F. & Bowring, S.A. An algorithm for U-Pb isotope dilution data reduction and uncertainty propagation. *Geochem. Geophys. Geosyst.* **12**, Q0AA18 (2011)
15. Münker, C., Weyer, S., Scherer, E. & Mezger, K. Separation of high field strength elements (Nb, Ta, Zr, Hf) and Lu from rock samples for MC-ICPMS measurements. *Geochem. Geophys. Geosyst.* **2**, doi:10.1029/2001gc000183 (2001).
16. Neumann,W. and Huster, E. Discussion of the 87Rb half-life determined by absolute counting. *Earth Planet. Sci. Lett.* **33**, 277–88 (1976).
17. Peucker-Ehrenbrink, B., Hofmann, A. W. & Hart, S. R. Hydrothermal lead transfer from mantle to continental crust: the role of metalliferous sediments. *Earth Planet. Sci. Lett.* **125**, 129-142 (1994).
18. Plank, T. in *Treatise on Geochemistry (Second Edition)* (eds Heinrich D. Holland & Karl K. Turekian) 607-629 (Elsevier, 2014).
19. Scherer, E., Munker, C. and Mezger, K. Calibration of the lutetium-hafnium clock. Science **293**, 683–688 (2001).
20. Skora, S. & Blundy, J. High-pressure Hydrous Phase Relations of Radiolarian Clay and Implications for the Involvement of Subducted Sediment in Arc Magmatism. *J. Petrol.* **51**, 2211-2243 (2010).
21. Tanaka, T. *et al.* JNdi-1: a neodymium isotopic reference in consistency with LaJolla neodymium. *Chem. Geo.* **168**, 279-281 (2000).
22. Vervoort, J. D., Plank, T. & Prytulak, J. The Hf-Nd isotopic composition of marine sediments. *Geochim. Cosmochim. Acta.* **75**, 5903-5926 (2011).

23. Weis, D. *et al.* High-precision isotopic characterization of USGS reference materials by TIMS and MC-ICP-MS. *Geochem. Geophys. Geosyst.* **7**, doi:10.1029/2006gc001283 (2006).
24. Weis, D. et al. Hf isotope compositions of US Geological Survey reference materials. *Geochem. Geophys. Geosyst.* **8**, doi:10.1029/2006gc001473 (2007).

8. Additional references for the literature data shown in the figures:

1. Brophy, J. G. Andesites from northeastern Kanaga island, Aleutians - implications for calc-alkaline fractionation mechanisms and magma chamber development. *Contrib. Mineral. Petrol.* **104**, 568-581, doi:10.1007/bf00306665 (1990).
2. Byers, F. M., Jr. Geology of Umnak and Bogoslof Islands, Aleutian Islands, Alaska. *U.S.G.S. Bull.* **1028-L**, 263-369 (1959).
3. Coats, R.R. Geology of Northern Adak Island, Alaska: *U.S.G.S. Bull.* **1028-C**, 45-67 (1956a).
4. Coats, R.R. Geology of northern Kanaga Island, Alaska: *U.S.G.S. Bull.* **1028-D**, 69-81 (1956b).
5. Coats, R.R. Reconnaissance geology of some western Aleutian Islands, Alaska: *U.S.G.S. Bull.* **1028-E**, 100 (1956c).
6. Coats, R.R., Nelson, W.H., Lewis, R.Q. and Powers, H.A. Geologic reconnaissance of Kiska Island, Aleutian Islands, Alaska: *U.S.G.S. Bull.* **1028-R**, 563-581 (1961).
7. Citron, G. P., Kay, R. W., Kay, S. M., Snee, L. W. & Sutter, J. F. Tectonic significance of early oligocene plutonism on Adak island, central Aleutian islands, Alaska. *Geology* **8**, 375-379 (1980).
8. Conrad, W.K. & Kay, R.W. Ultramafic and mafic inclusions from Adak Island: Crystallization history and implications for the nature of primary magmas and crustal evolution in the Aleutian Arc. *J. Petrol.* **25**, 88-125 (1984).
9. Delong, S. E., Perfit, M. R., McCulloch, M. T. & Ach, J. Magmatic evolution of Semisopochnoi island, Alaska - trace element and isotopic constraints. *J. Geol.* **93**, 609-618 (1985).
10. Delong, S. E. Distribution of Rb, Sr and Ni in igneous rocks, central and western Aleutian-islands Alaska. *Geochim. Cosmochim. Acta* **38**, 245-266 (1974).
11. Drewes, H., Fraser, G.D., Snyder, G.L. and Barnett, H.F.J. Geology of Unalaska Island and adjacent insular shelf, Aleutian Islands, Alaska: *U.S.G.S. Bull.* **1028-S**, 583-676 (1961).
12. Fraser, G.D. and Barrett, H.F. Geology of the Delarof and westernmost Andreanof Islands, Alaska: *U.S.G.S. Bull.* **1028-I**, 211-245 (1959).
13. Gates, O. P., H.A.; Wilcox, R.E.; Schafer, J.P. Geology of the Near Islands, Alaska. *U.S.G.S. Bull.* **1028-U**, 709-822 (1971).
14. George, R. *et al.* Melting processes and fluid and sediment transport rates along the Alaska-Aleutian arc from an integrated U-Th-Ra-Be isotope study. *J. Geophys. Res.* **108**, doi:10.1029/2002jb001916 (2003).
15. Gust, D. A. & Perfit, M. R. Phase relations of a high-Mg basalt from the Aleutian Island Arc: Implications for primary island arc basalts and high-Al basalts. *Contrib. Mineral. Petrol.* **97**, 7-18 (1987).

16. Jicha, B.R., Singer, B.S., Brophy, J.G., Fournelle, J.H., Johnson, C.M., Beard, B.L., Lapen, T.J., Mahlen, N.J. Variable impact of the subducted slab on Aleutian island arc magma sources: evidence from Sr, Nd, Pb, and Hf isotopes and trace element abundances. Journal of Petrology 45 (9), 1845–1875 (2004).
17. Kay, S. M. Metamorphism in the Aleutian arc - the Finger Bay pluton, Adak, Alaska. *Canadian Mineralogist* **21**, 665-681 (1983).
18. Kay, S. M., Kay, R. W., Citron, G. P. & Perfit, M. R. Calc-alkaline plutonism in the intra-oceanic Aleutian arc, Alaska. *Geol. Soc. Amer. Spec. Papers* **241**, 233-256 (1990).
19. Kay, R. W. & Mahlburg Kay, S. Delamination and delamination magmatism. *Tectonophysics* **219**, 177-189 (1993).
20. McCulloch, M. T. & Perfit, M. R. 143Nd/144Nd, 87Sr/86Sr and trace element constraints on the petrogenesis of Aleutian island arc magmas. *Earth Planet. Sci. Lett.* **56**, 167-179 (1981).
21. Myers, J. D. & Frost, C. D. A petrologic re-investigation of the Adak volcanic center, central Aleutian arc, Alaska. *J. Volcanol. Geotherm. Res.* **60**, 109-146 (1994).
22. Myers, J.D., Marsh, B.D. and Sinha, A.K. Strontium isotopic and selected trace-element variations between 2 Aleutian volcanic centers (Adak and Atka) – Implications for the development of arc volcanic plumbing systems: *Contrib. Mineral. Petrol.* **91**, 221-234 (1985)
23. Myers, J. D., Marsh, B. D., Frost, C. D. & Linton, J. A. Petrologic constraints on the spatial distribution of crustal magma chambers, Atka Volcanic Center, central Aleutian arc. *Contrib. Mineral. Petrol.* **143**, 567-586 (2002).
24. Nye, C. J. & Reid, M. R. Geochemistry of primary and least fractionated lavas from Okmok Volcano, Central Aleutians: Implications for arc magmagenesis. *J. Geophys. Res.* **91**, 10271 (1986).
25. Nye, C. J., Swanson, S. E., Avery, V. F. & Miller, T. P. Geochemistry of the 1989–1990 eruption of redoubt volcano: Part I. Whole-rock major- and trace-element chemistry. *J. Volcanol. Geotherm. Res.* **62**, 429-452 (1994).
26. Romick, J. D., Perfit, M. R., Swanson, S. E. & Shuster, R. D. Magmatism in the eastern Aleutian Arc: temporal characteristic of igneous activity on Akutan Island. *Contrib. Mineral. Petrol.* **104**, 700-721 (1990).
27. Singer, B. S., Myers, J. D. & Frost, C. D. Mid-Pleistocene lavas from the Seguam volcanic center, central Aleutian arc: closed-system fractional crystallization of a basalt to rhyodacite eruptive suite. *Contrib. Mineral. Petrol.* **110**, 87-112 (1992).
28. The Aleutian Arc website, website hosted by the Department of Geology and Geophysics, University of Wyoming, http://www.gg.uwyo.edu/aleutians/index.htm (accessed June 2006).
29. Tsvetkov, A. A. Magmatism of the westernmost (Komandorsky) segment of the Aleutian Island Arc. *Tectonophysics* **199**, 289-317 (1991).
30. von Drach, V., Marsh, B. D. & Wasserburg, G. J. Nd and Sr isotopes in the Aleutians - multicomponent parenthood of island-arc magmas. *Contrib. Mineral. Petrol.* **92**, 13-34 (1986).